

**The protonmotive force and respiratory control:**

**Building blocks of mitochondrial physiology**

**Part 1.**

[http://www.mitoeagle.org/index.php/MitoEAGLE\\_preprint\\_2017-09-21](http://www.mitoeagle.org/index.php/MitoEAGLE_preprint_2017-09-21)

Preprint version 08 (2017-10-11)

**MitoEAGLE Network**

Corresponding author: Gnaiger E

Contributing co-authors

Ahn B, Alves MG, Amati F, Åsander Frostner E, Battino M, Beard DA, Ben-Shachar D, Bishop D, Breton S, Brown GC, Brown RA, Buettner GR, Cervinkova Z, Chicco AJ, Coen PM, Collins JL, Crisóstomo L, Davis MS, Dias T, Distefano G, Doerrier C, Ehinger J, Elmer E, Fell DA, Filipovska A, Fisher J, Garcia-Roves PM, Garcia-Souza LF, Genova ML, Gonzalo H, Goodpaster BH, Gorr TA, Han J, Harrison DK, Hellgren KT, Hernansanz P, Holland O, Hoppel CL, Iglesias-Gonzalez J, Irving BA, Iyer S, Jansen-Dürr P, Jespersen NR, Jha RK, Käämbre T, Kane DA, Kappler L, Keijer J, Komlodi T, Krako Jakovljevic N, Kuang J, Labieniec-Watala M, Lai N, Laner V, Lee HK, Lemieux H, Lerfall J, Lucchinetti E, MacMillan-Crow LA, Makrecka-Kuka M, Meszaros AT, Moiso N, Molina AJA, Montaigne D, Moore AL, Murray AJ, Newsom S, Nozickova K, O'Gorman D, Oliveira PF, Oliveira PJ, Orynbayeva Z, Pak YK, Palmeira CM, Patel HH, Pesta D, Petit PX, Pichaud N, Pirkmajer S, Porter RK, Pranger F, Prochownik EV, Radenkovic F, Reboredo P, Renner-Sattler K, Robinson MM, Rohlena J, Røslund GV, Rossiter HB, Salvadego D, Scatena R, Schartner M, Scheibye-Knudsen M, Schilling JM, Schlattner U, Schoenfeld P, Scott GR, Singer D, Sobotka O, Spinazzi M, Stocker R, Sumbalova Z, Suravajhala P, Tanaka M, Tandler B, Tepp K, Tomar D, Towheed A, Trivigno C, Tronstad KJ, Tyrrell DJ, Velika B, Vendelin M, Vercesi

27 AE, Victor VM, Ward ML, Watala C, Wei YH, Wieckowski MR, Wohlwend M, Wolff J,  
28 Wuest RCI, Zaugg M, Zorzano A

29

30 Supporting co-authors:

31 Arandarčikaitė O, Bailey DM, Bakker BM, Batista Ferreira J, Bernardi P, Boetker HE,

32 Borsheim E, Borutaitė V, Bouitbir J, Calabria E, Calbet JA, Carvalho E, Chaurasia B,

33 Clementi E, Coker RH, Collin A, Das AM, De Palma C, Dubouchaud H, Duchon MR,

34 Durham WJ, Dyrstad SE, Engin AB, Fornaro M, Gan Z, Garlid KD, Garten A, Gourlay CW,

35 Granata C, Haas CB, Haavik J, Haendeler J, Hand SC, Hepple RT, Hickey AJ, Hoel F,

36 Kainulainen H, Keppner G, Khamoui AV, Klingenspor M, Koopman WJH, Kowaltowski AJ,

37 Krajcova A, Lenaz G, Malik A, Markova M, Mazat JP, Menze MA, Methner A, Muntané J,

38 Muntean DM, Neuzil J, Oliveira MT, Pallotta ML, Parajuli N, Pettersen IKN, Pulinilkunnil T,

39 Ropelle ER, Salin K, Sandi C, Sazanov LA, Siewiera K, Silber AM, Skolik R, Smenes BT,

40 Soares FAA, Sokolova I, Sonkar VK, Stankova P, Stier A, Swerdlow RH, Szabo I, Trifunovic

41 A, Thyfault JP, Tretter L, Trougakos IP, Vieyra A, Votion DM, Williams C, Zaugg K

42

43 **Updates:**

44 [http://www.mitoeagle.org/index.php/MitoEAGLE\\_preprint\\_2017-09-21](http://www.mitoeagle.org/index.php/MitoEAGLE_preprint_2017-09-21)

45

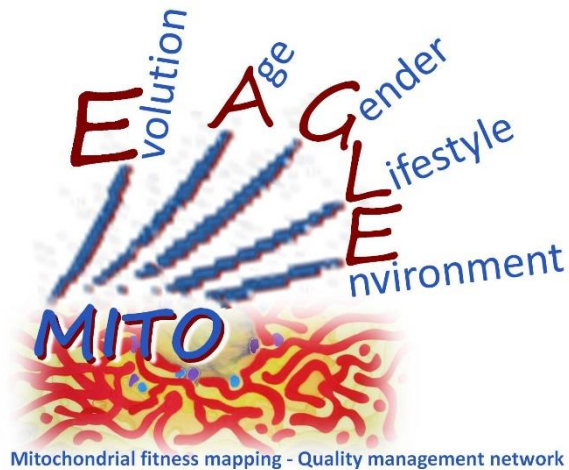
Correspondence: Gnaiger E

Department of Visceral, Transplant and Thoracic Surgery, D. Swarovski Research Laboratory, Medical University of Innsbruck, Innrain 66/4, A-6020 Innsbruck, Austria

Email: [erich.gnaiger@i-med.ac.at](mailto:erich.gnaiger@i-med.ac.at)

Tel: +43 512 566796, Fax: +43 512 566796 20

This manuscript on 'The protonmotive force and respiratory control' is a position statement in the frame of COST Action CA15203 MitoEAGLE. The list of co-authors evolved from MitoEAGLE Working Group Meetings and a **bottom-up** spirit of COST in phase 1: This is an open invitation to scientists and students to join as co-authors, to provide a balanced view on mitochondrial respiratory control, a fundamental introductory presentation of the concept of the protonmotive force, and a consensus statement on reporting data of mitochondrial respiration in terms of metabolic flows and fluxes. We plan a series of follow-up reports by the expanding MitoEAGLE Network, to increase the scope of recommendations on harmonization and facilitate global communication and collaboration.



Phase 2 - until **October 12**: We continue to invite comments and suggestions on the MitoEAGLE preprint, particularly if you are an **early career investigator adding an open future-oriented perspective**, or an **established scientist providing a balanced historical basis**. Your critical input into the quality of the manuscript will be most welcome, improving our aims to be educational, general, consensus-oriented, and practically helpful for students working in mitochondrial respiratory physiology.

To join as a co-author, please feel free to focus on a particular section in terms of direct input and references, contributing to the scope of the manuscript from the perspective of your expertise. Your comments will be largely posted on the discussion page of the MitoEAGLE preprint website.

If you prefer to submit comments in the format of a referee's evaluation rather than a contribution as a co-author, I will be glad to distribute your views to the updated list of co-authors for a balanced response. We would ask for your consent on this open bottom-up policy.

We organize a MitoEAGLE session linked to our series of reports at the MiPconference Nov 2017 in Hradec Kralove in close association with the MiPsociety (where you hopefully will attend) and at EBEC 2018 in Budapest.

» [http://www.mitoeagle.org/index.php/MiP2017\\_Hradec\\_Kralove\\_CZ](http://www.mitoeagle.org/index.php/MiP2017_Hradec_Kralove_CZ)

I thank you in advance for your feedback.

With best wishes,

Erich Gnaiger

Chair Mitochondrial Physiology Society - <http://www.mitophysiology.org>

Chair COST Action MitoEAGLE - <http://www.mitoeagle.org>

Medical University of Innsbruck, Austria

|     |   |
|-----|---|
| 95  | <b>Contents</b>   |
| 96  | <b>1. Introduction</b>  |
| 97  | <b>2. Respiratory coupling states in mitochondrial preparations</b>                             |
| 98  | Mitochondrial preparations  |
| 99  | 2.1. <i>Three coupling states of mitochondrial preparations and residual oxygen consumption</i> |
| 100 | Coupling control states   |
| 101 | Respiratory capacities and kinetic control  |
| 102 | Phosphorylation, P <sub>o</sub>   |
| 103 | LEAK, OXPHOS, ET, ROX   |
| 104 | 2.2. <i>Coupling states and respiratory rates</i>   |
| 105 | 2.3. <i>Classical terminology for isolated mitochondria</i>                                     |
| 106 | States 1-5  |
| 107 | <b>3. The protonmotive force and proton flux</b>  |
| 108 | 3.1. <i>Electric and chemical partial forces versus electrical and chemical units</i>           |
| 109 | Faraday constant  |
| 110 | Electrical part of the protonmotive force   |
| 111 | Chemical part of the protonmotive force   |
| 112 | 3.2. <i>Definitions</i>   |
| 113 | Control and regulation  |
| 114 | Respiratory control and response  |
| 115 | Respiratory coupling control  |
| 116 | Pathway control states  |
| 117 | The steady-state  |
| 118 | 3.3. <i>Forces and fluxes in physics and irreversible thermodynamics</i>                        |
| 119 | Vectorial and scalar forces, and fluxes   |
| 120 | Coupling  |
| 121 | Coupled versus bound processes  |
| 122 | <b>4. Normalization: fluxes and flows</b>   |
| 123 | 4.1. <i>Flux per chamber volume</i>   |
| 124 | 4.2. <i>System-specific and sample-specific normalization</i>                                   |
| 125 | Extensive quantities  |
| 126 | Size-specific quantities  |
| 127 | Molar quantities  |
| 128 | Flow per system, $I$  |
| 129 | Size-specific flux, $J$   |
| 130 | Sample concentration, $C_{mX}$  |
| 131 | Mass-specific flux, $J_{mX,O_2}$  |
| 132 | Number concentration, $C_{NX}$  |
| 133 | Flow per sample entity, $I_{X,O_2}$   |
| 134 | 4.3. <i>Normalization for mitochondrial content</i>   |
| 135 | Mitochondrial concentration, $C_{mte}$ , and mitochondrial markers                              |
| 136 | Mitochondria-specific flux, $J_{mte,O_2}$   |
| 137 | 4.4. <i>Conversion: units and normalization</i>   |
| 138 | 4.5. <i>Conversion: oxygen, proton and ATP flux</i>   |
| 139 | <b>5. Conclusions</b>   |
| 140 | <b>6. References</b>  |
| 141 |   |

142 **Abstract**

143 Clarity of concept and consistency of nomenclature are key trademarks of a research field.  
144 These trademarks facilitate effective transdisciplinary communication, education, and  
145 ultimately further discovery. As the knowledge base and importance of mitochondrial  
146 physiology to human health expand, the necessity for harmonizing nomenclature concerning  
147 mitochondrial respiratory states and rates has become increasingly apparent. Peter Mitchell's  
148 concept of the protonmotive force establishes the links between electrical and chemical  
149 components of energy transformation and coupling in oxidative phosphorylation. This unifying  
150 concept provides the framework for developing a consistent nomenclature for mitochondrial  
151 physiology and bioenergetics. Herein, we follow IUPAC guidelines on general terms of  
152 physical chemistry, extended by the concepts of open systems and irreversible thermodynamics.  
153 We align the nomenclature of classical bioenergetics on respiratory states with a concept-driven  
154 constructive terminology to address the meaning of each respiratory state. Furthermore, we  
155 suggest uniform standards for the evaluation of respiratory states that will ultimately support  
156 the development of databases of mitochondrial respiratory function in species, tissues and cells  
157 studied under diverse physiological and experimental conditions. In this position statement, in  
158 the frame of COST Action CA15203 MitoEAGLE, we endeavour to provide a balanced view  
159 on mitochondrial respiratory control, a fundamental introductory presentation of the concept of  
160 the protonmotive force, and a critical discussion on reporting data of mitochondrial respiration  
161 in terms of metabolic flows and fluxes.

162

163 *Keywords:* Mitochondrial respiratory control, coupling control, mitochondrial  
164 preparations, protonmotive force, chemiosmotic theory, oxidative phosphorylation, OXPHOS,  
165 efficiency, electron transfer, ET; proton leak, LEAK, residual oxygen consumption, ROX, State  
166 2, State 3, State 4, normalization, flow, flux

167

168

169 **Box 1:**

170

171 **In brief:**172 **mitochondria**173 **and Bioblasts**

\* Does the public expect biologists to understand Darwin's theory of evolution?

\* Do students expect that researchers of bioenergetics can explain Mitchell's theory of chemiosmotic energy transformation?

174 **Mitochondria** were described for the first time in 1857 by Rudolph Albert von Kölliker as

175 granular structures or 'sarkosomes'. In 1886 Richard Altman called them 'bioblasts' (published

176 1894). The word 'mitochondrium' (Greek mitos: thread; chondros: granule) was introduced by

177 Carl Benda (1898). Mitochondria are the oxygen consuming electrochemical generators which

178 evolved from endosymbiotic bacteria (Margulis 1970). The bioblasts of Richard Altmann

179 (1894) include not only the mitochondria, but also symbiotic and free-living bacteria. We now

180 recognize mitochondria as dynamic organelles with a double membrane that are contained

181 within eukaryotic cells. The inner mitochondrial membrane shows dynamic tubular and disk-

182 shaped cristae that separate the mitochondrial matrix, *i.e.* the internal mitochondrial

183 compartment, and the intermembrane space; the latter being enclosed by the outer

184 mitochondrial membrane. Mitochondria are the structural and functional elemental units of cell

185 respiration, where cell respiration is defined as the consumption of oxygen coupled to

186 electrochemical proton translocation across the inner mitochondrial membrane. In the process

187 of oxidative phosphorylation (OXPHOS), the reduction of O<sub>2</sub> is electrochemically coupled to

188 the transformation of energy in the form of ATP (Mitchell 2011). These powerhouses of the

189 cell contain the machinery of the OXPHOS pathway, including transmembrane respiratory

190 complexes (*i.e.* FMN, Fe-S and cytochrome *b*, *c*, *aa*<sub>3</sub> redox systems), alternative

191 dehydrogenases and oxidases, the coenzyme ubiquinone (coenzyme Q) and ATP synthase

192 together with the enzymes of the tricarboxylic acid cycle and the fatty acid oxidation enzymes,

193 ion transporters, including substrate, co-factor and metabolite transporters as well as proton

194 pumps, and mitochondrial kinases related to energy transfer pathways. The mitochondrial

195 proteome comprises over 1,200 proteins (Mitocharta), mostly encoded by nuclear DNA

196 (nDNA), with a variety of functions, many of which are relatively well known (*e.g.* apoptosis-  
197 regulating proteins), are still under investigation, or need to be identified (alanine transporter).  
198 Mitochondria typically maintain several copies of their own genome (hundred to thousands per  
199 cell) which is maternally inherited and known as mitochondrial DNA (mtDNA). One exception  
200 to strictly maternal inheritance in animals is found in bivalves (Breton *et al.* 2007). mtDNA is  
201 16.5 Kb in length, contains 13 protein-coding genes for subunits of the transmembrane  
202 respiratory Complexes CI, CIII, CIV and ATP synthase, and also encodes 22 tRNAs and the  
203 mitochondrial 16S and 12S rRNA. The mitochondrial genome is both regulated and  
204 supplemented by nuclear-encoded mitochondrial targeted proteins. Evidence has accumulated  
205 that additional gene content is encoded in the mitochondrial genome, *e.g.* microRNAs, piRNA,  
206 smithRNAs, repeat associated RNA, and even additional proteins (Duarte *et al.* 2014; Lee *et*  
207 *al.* 2015; Cobb *et al.* 2016). The inner mitochondrial membrane contains the non-bilayer  
208 phospholipid cardiolipin, which is not present in any other eukaryotic cellular membrane.  
209 Cardiolipin promotes the formation of respiratory supercomplexes, which are supramolecular  
210 assemblies based upon specific, though dynamic, interactions between individual respiratory  
211 complexes (Greggio *et al.* 2017; Lenaz *et al.* 2017). There is a constant crosstalk between  
212 mitochondria and the other cellular components at the transcriptional or post-translational level,  
213 and through cell signalling in response to varying energy demands (Quiros *et al.* 2016). In  
214 addition to mitochondrial movement along the microtubules, mitochondrial morphology can  
215 change in response to energy requirements of the cell via processes known as fusion and fission  
216 through which mitochondria can communicate within a network, and in various pathological  
217 states which cause swelling or dysregulation of fission and fusion. Mitochondrial dysfunction  
218 is associated with a wide variety of genetic and degenerative diseases. Therefore, a better  
219 understanding of mitochondrial physiology will improve our understanding of the etiology of  
220 disease and the diagnostic repertoire of mitochondrial medicine. Abbreviation: mt, as generally  
221 used in mtDNA. Mitochondrion is singular and mitochondria is plural.

222 *‘For the physiologist, mitochondria afforded the first opportunity for an experimental*  
223 *approach to structure-function relationships, in particular those involved in active transport,*  
224 *vectorial metabolism, and metabolic control mechanisms on a subcellular level’ (Ernster and*  
225 *Schatz 1981).*

---

226

## 227 **1. Introduction**

228 Mitochondria are the powerhouses of the cell with numerous physiological, molecular,  
229 and genetic functions (**Box 1**). Every study of mitochondrial function and disease is faced with  
230 **E**volution, **A**ge, **G**ender and sex, **L**ifestyle, and **E**nvironment (EAGLE) as essential background  
231 conditions intrinsic to the individual patient or subject, cohort, species, tissue and to some extent  
232 even cell line. As a large and highly coordinated group of laboratories and researchers, the  
233 mission of the global MitoEAGLE Network is to generate the necessary scale, type, and quality  
234 of consistent data sets and conditions to address this intrinsic complexity. Harmonization of  
235 experimental protocols and implementation of a quality control and data management system  
236 is required to interrelate results gathered across a spectrum of studies and to generate a  
237 rigorously monitored database focused on mitochondrial respiratory function. In this way,  
238 researchers within the same and across different disciplines will be positioned to compare their  
239 findings to an agreed upon set of clearly defined and accepted international standards.

240 Reliability and comparability of quantitative results depend on the accuracy of  
241 measurements under strictly-defined conditions. A conceptually clearly-defined framework is  
242 also required to warrant meaningful interpretation and comparability of experimental outcomes  
243 carried out by research groups at different institutes. With an emphasis on quality of research,  
244 collected data can be useful far beyond the specific question of a specific experiment. Vague or  
245 ambiguous jargon can lead to confusion and may relegate valuable signals to wasteful noise.  
246 For this reason, measured values must be expressed in standardized units for each parameter  
247 used to define mitochondrial respiratory function. Standardization of nomenclature and



248 technical terms is essential to improve the awareness of the intricate meaning of divergent  
249 scientific vocabulary. The focus on coupling states, the protonmotive force and fluxes through  
250 metabolic pathways of aerobic energy transformation in mitochondrial preparations is a first  
251 step in the attempt to generate a harmonized and conceptually oriented nomenclature in  
252 bioenergetics and mitochondrial physiology. Coupling states of intact cells and respiratory  
253 control by fuel substrates and specific inhibitors of respiratory enzymes will be reviewed in  
254 subsequent communications.

255

## 256 **2. Respiratory coupling states in mitochondrial preparations**

257 *‘Every professional group develops its own technical jargon for talking about*  
258 *matters of critical concern ... People who know a word can share that idea with*  
259 *other members of their group, and a shared vocabulary is part of the glue that holds*  
260 *people together and allows them to create a shared culture’ (Miller 1991).*

261

262 **Mitochondrial preparations** are defined as either isolated mitochondria, or tissue and  
263 cellular preparations in which the barrier function of the plasma membrane is disrupted. The  
264 plasma membrane separates the cytosol, nucleus and organelles (the intracellular compartment)  
265 from the environment of the cell. The plasma membrane consists of a lipid bilayer, embedded  
266 proteins and attached organic molecules which collectively control the selective permeability  
267 of ions, organic molecules and particles across the cell boundary. The intact plasma membrane,  
268 therefore, prevents the passage of many water-soluble mitochondrial substrates, such as  
269 succinate or ADP, that are required for the analysis of respiratory capacity at kinetically  
270 saturating concentrations, thus limiting the scope of investigations into mitochondrial  
271 respiratory function in intact cells. The cholesterol content of the plasma membrane is high  
272 compared to mitochondrial membranes. Therefore, mild detergents, such as digitonin and  
273 saponin, can be applied to selectively permeabilize the plasma membrane by interaction with

274 cholesterol and allow free exchange of cytosolic components with ions and organic molecules  
275 of the immediate cell environment, while maintaining the integrity and localization of  
276 organelles, cytoskeleton and the nucleus. Application of optimum concentrations of these mild  
277 detergents leads to the complete loss of cell viability, tested by nuclear staining, while  
278 mitochondrial function remains unaffected, as shown by an unaltered respiration rate of  
279 mitochondria after the addition of such low concentrations of digitonin and saponin. In addition  
280 to mechanical permeabilization during homogenization of fresh tissue, saponin may be applied  
281 to ensure permeabilization of all cells. Crude homogenate and cells permeabilized in the  
282 respiration chamber contain all components of the cell at highly diluted concentrations. All  
283 mitochondria are retained in chemically permeabilized mitochondrial preparations and crude  
284 tissue homogenates. In the preparation of isolated mitochondria, the cells or tissues are  
285 homogenized, and the mitochondria are separated from other cell fractions and purified by  
286 centrifugation, entailing the loss of a significant fraction of mitochondria. The term  
287 mitochondrial preparation does not include further fractionation of mitochondrial components,  
288 as well as submitochondrial particles.

289

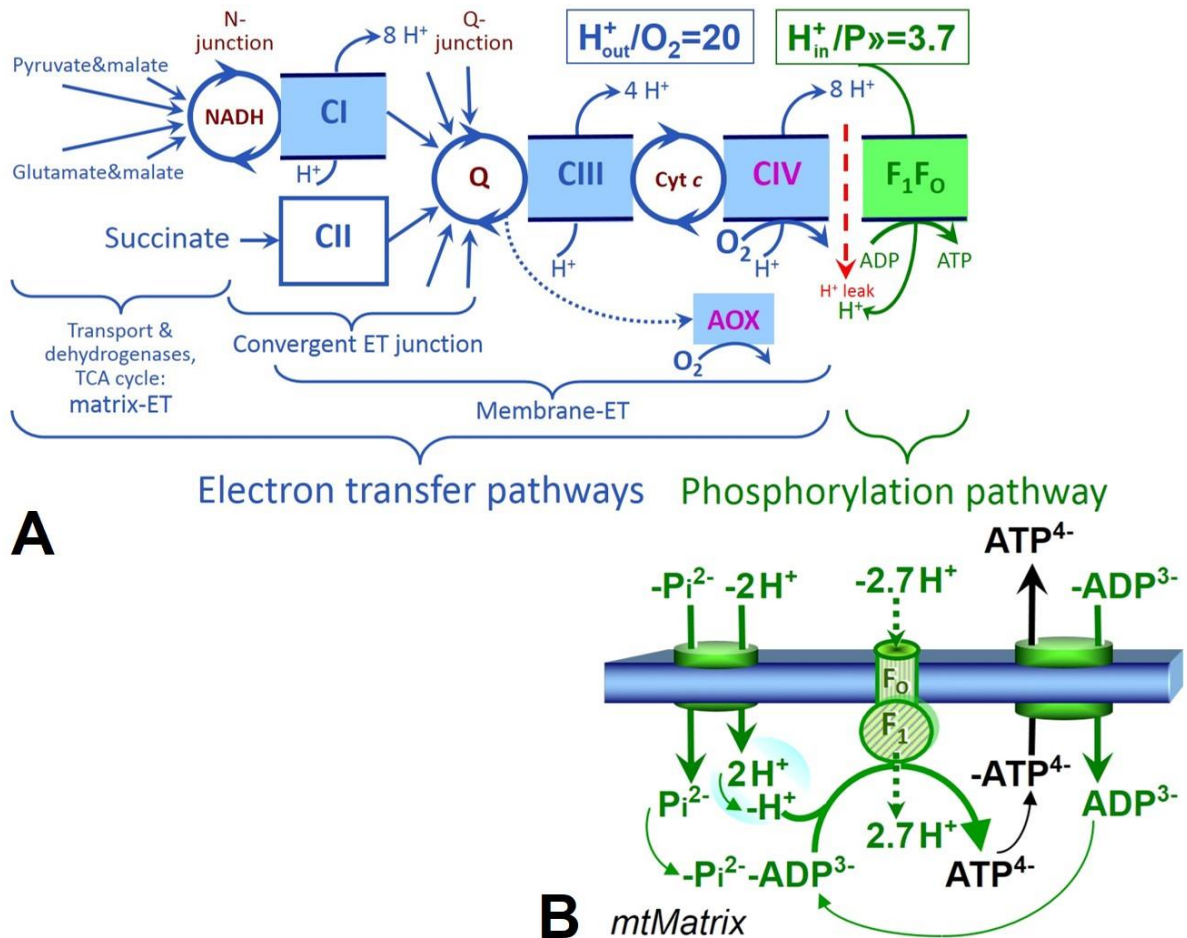
### 290 *2.1. Three coupling states of mitochondrial preparations and residual oxygen consumption*

291 **Coupling control states:** To extend the classical nomenclature on mitochondrial  
292 coupling states (Section 2.4) by a concept-driven terminology that incorporates explicit  
293 information on the nature of the respiratory states, the terminology must be general and not  
294 restricted to any particular experimental protocol or mitochondrial preparation (Gnaiger 2009).  
295 We focus primarily on the conceptual ‘why’, along with clarification of the experimental ‘how’.  
296 In the following section, the concept-driven terminology is explained and coupling states are  
297 defined. To provide a diagnostic reference for respiratory capacities of core energy metabolism,  
298 the capacity of *oxidative phosphorylation*, OXPHOS, is measured at kinetically saturating  
299 concentrations of ADP and inorganic phosphate,  $P_i$ . The *oxidative* capacity of the electron

300 transfer-pathway, ET-pathway, reveals the limitation of OXPHOS capacity mediated by the  
301 *phosphorylation* pathway. The ET and phosphorylation pathways comprise coupled segments  
302 of the OXPHOS pathway. ET capacity is measured as noncoupled respiration by application of  
303 *external uncouplers*. The contribution of *intrinsically uncoupled* oxygen consumption is most  
304 easily studied by not stimulating or arresting phosphorylation, when oxygen consumption  
305 compensates mainly for the proton leak; the corresponding states are collectively classified as  
306 LEAK states (**Table 1**). Fuel substrates and ET inhibitors are kept constant, *i.e.* maintaining a  
307 defined ET-pathway state, while (1) adding ADP or P<sub>i</sub>, (2) inhibiting the phosphorylation  
308 pathway, and (3) performing uncoupler titrations to induce different coupling states (**Fig. 1**).

309 **Respiratory capacities and kinetic control:** Coupling control states are established in  
310 the study of mitochondrial preparations to obtain reference values for various output variables.  
311 Physiological conditions *in vivo* may deviate substantially from these experimentally obtained  
312 states. Since kinetically saturating concentrations, *e.g.* of ADP or oxygen, may not apply to  
313 physiological intracellular conditions, relevant information is obtained in studies of kinetic  
314 responses to conditions intermediate between the LEAK state at zero [ADP] and the OXPHOS  
315 state at saturating [ADP], or of respiratory capacities in the range between kinetically saturating  
316 [O<sub>2</sub>] and anoxia (Gnaiger 2001). We define respiratory capacities, comparable to channel  
317 capacity in information theory, as the upper bound of the rate of respiration measured in defined  
318 coupling and pathway control states of mitochondrial preparations.

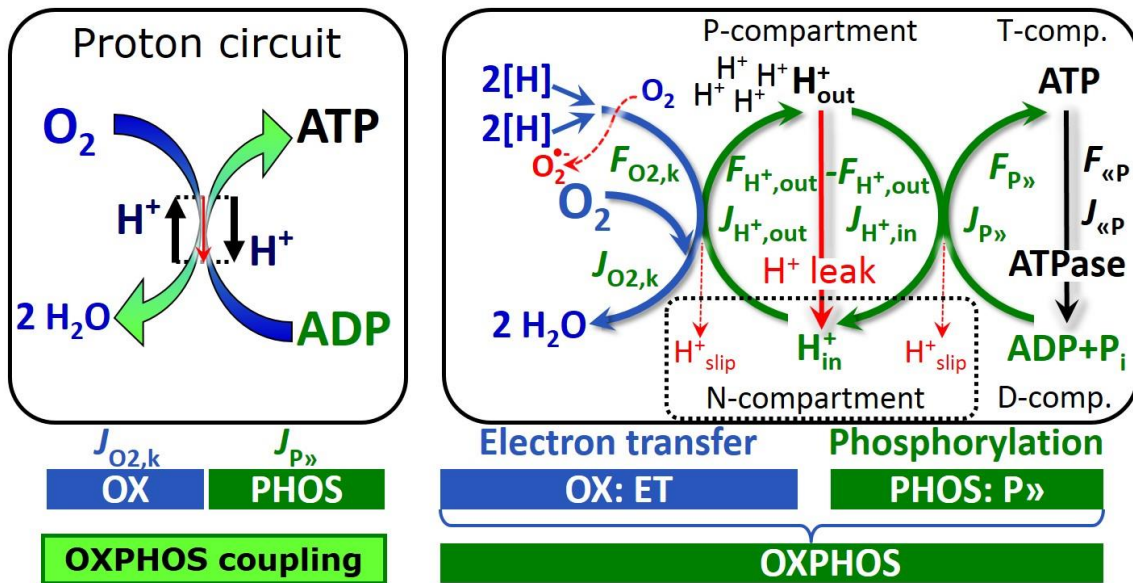
319



320

321 **Fig. 1. The oxidative phosphorylation pathway, OXPHOS pathway.** (A) Electron transfer, ET,  
 322 coupled to phosphorylation. Multiple convergent electron transfer pathways are shown from NADH and  
 323 succinate; additional arrows indicate electron entry through electron transferring flavoprotein,  
 324 glycerophosphate dehydrogenase, dihydro-orotate dehydrogenase, choline dehydrogenase, and  
 325 sulfide-ubiquinone oxidoreductase. The branched pathway of oxygen consumption by alternative quinol  
 326 oxidase (AOX) is indicated by the dotted arrow.  $H^+_{out}/O_2$  is the ratio of outward proton flux from the matrix  
 327 space to catabolic  $O_2$  flux in the NADH-linked pathway.  $H^+_{in}/P \gg$  is the ratio of inward proton flux from the  
 328 inter-membrane space to the flux of phosphorylation of ADP to ATP. Due to proton leak and slip these  
 329 are not fixed stoichiometries. (B) Phosphorylation pathway catalyzed by the F<sub>1</sub>F<sub>0</sub> ATP synthase,  
 330 adenine nucleotide translocase, and inorganic phosphate transporter. The  $H^+_{in}/P \gg$  stoichiometry is the  
 331 sum of the coupling stoichiometry in the ATP synthase reaction (-2.7 H<sup>+</sup> from the intermembrane space,  
 332 2.7 H<sup>+</sup> to the matrix) and the proton balance in the translocation of ADP<sup>2-</sup>, ATP<sup>3-</sup> and Pi<sup>2-</sup>. See Eqs. 3  
 333 and 4 for further explanation. Modified from (A) Lemieux *et al.* (2017) and (B) Gnaiger (2014).

334



335

336

337

338

339

340

341

342

343

344

345

346

347

348

349

350

351

352

353

354

**Fig. 2. The proton circuit and coupling in oxidative phosphorylation (OXPHOS).** Oxygen flux,  $J_{O_2,k}$ , through the catabolic electron transfer (ET) pathway  $k$  is coupled to flux through the phosphorylation pathway of ADP to ATP,  $J_{P\gg}$ , by the proton pumps of the ET-pathway, pushing the outward proton flux,  $J_{H^+,out}$ , and generating the output protonmotive force,  $F_{H^+,out}$ . ATP synthase is coupled to inward proton flux,  $J_{H^+,in}$ , to phosphorylate ADP with inorganic phosphate to ATP, driven by the input protonmotive force,  $F_{H^+,in} = -F_{H^+,out}$ .  $2[H]$  indicates the reduced hydrogen equivalents of fuel substrates that provide the chemical input force,  $F_{O_2,k}$  [kJ/mol  $O_2$ ], of the catabolic reaction  $k$  with oxygen (Gibbs energy of reaction per mole  $O_2$  consumed in reaction  $k$ ), typically in the range of -460 to -480 kJ/mol. The output force is given by the phosphorylation potential difference (ADP phosphorylated to ATP),  $F_{P\gg}$ , which varies *in vivo* ranging from about 48 to 62 kJ/mol under physiological conditions. Fluxes,  $J_B$ , and forces,  $F_B$ , are expressed in either chemical units, [mol·s<sup>-1</sup>·m<sup>-3</sup>] and [J·mol<sup>-1</sup>] respectively, or electrical units, [C·s<sup>-1</sup>·m<sup>-3</sup>] and [J·C<sup>-1</sup>] respectively, per volume,  $V$  [m<sup>3</sup>], of the system. The system defined by the boundaries shown as a full black line is not a black box, but is analysed as a compartmental system. The negative compartment (N-compartment, enclosed by the dotted line) is the matrix space, separated from the positive compartment (P-compartment) by the inner mitochondrial membrane. ADP+P<sub>i</sub> and ATP are the substrate- and product-compartments (scalar D- and T-comp.), respectively. Chemical potentials of all substrates and products involved in the scalar reactions are measured in the P-compartment for calculation of the scalar forces  $F_{O_2,k}$  and  $F_{P\gg} = -F_{\ll P}$  (**Box 2**). Modified from Gnaiger (2014).

355        **Phosphorylation, P»:** *Phosphorylation* in the context of OXPHOS is defined as  
356 phosphorylation of ADP to ATP. On the other hand, the term phosphorylation is used generally  
357 in many different contexts, *e.g.* protein phosphorylation. This justifies consideration of a  
358 symbol more discriminating and specific than P as used in the P/O ratio (phosphate to atomic  
359 oxygen ratio), where P indicates phosphorylation of ADP to ATP or GDP to GTP. We propose  
360 the symbol P» for the endergonic direction of phosphorylation ADP→ATP, and likewise the  
361 symbol «P for the corresponding exergonic hydrolysis ATP→ADP (**Fig. 2; Box 3**). ATP  
362 synthase is the proton pump of the phosphorylation pathway (**Fig. 1B**). P» may also involve  
363 substrate-level phosphorylation as part of the tricarboxylic acid cycle (succinyl-CoA ligase)  
364 and phosphorylation of ADP catalyzed by phosphoenolpyruvate carboxykinase, adenylate  
365 kinase, creatine kinase, hexokinase and nucleoside diphosphate kinase (NDPK). Kinase cycles  
366 are involved in intracellular energy transfer and signal transduction for regulation of energy  
367 flux. In isolated mammalian mitochondria ATP production catalyzed by adenylate kinase,  
368  $2\text{ADP} \leftrightarrow \text{ATP} + \text{AMP}$ , proceeds without fuel substrates in the presence of ADP (Komlódi and  
369 Tretter 2017).  $J_{\text{P»}}/J_{\text{O}_2, \text{k}}$  (P»/O<sub>2</sub>) is two times the ‘P/O’ ratio of classical bioenergetics. The  
370 effective P»/O<sub>2</sub> ratio is diminished by: (1) the proton leak across the inner mitochondrial  
371 membrane from low pH in the P-phase to high pH in the N-phase (P, positive; N, negative); (2)  
372 cycling of other cations; (3) proton slip in the proton pumps when a proton effectively is not  
373 pumped; and (4) electron leak in the univalent reduction of oxygen (O<sub>2</sub>; dioxygen) to superoxide  
374 anion radical (O<sub>2</sub><sup>•-</sup>).

375

376

377

378

379

380

381 **Table 1. Coupling states and residual oxygen consumption in mitochondrial**  
 382 **preparations in relation to respiration and phosphorylation rate,  $J_{O_2,k}$  and  $J_{P\gg}$ ,**  
 383 **and protonmotive force,  $F_{H^+,out}$ .** Coupling states are established at kinetically  
 384 saturating concentrations of fuel substrates and  $O_2$ .

| State  | $J_{O_2,k}$                                 | $J_{P\gg}$ | $F_{H^+,out}$ | Inducing factors  | Limiting factors  |
|--------|---|------------|---------------|---|---|
| LEAK   | $L$ ; low proton leak-dependent respiration | 0          | max.          | Proton leak, slip, and cation cycling                         | $J_{P\gg}=0$ : (1) without ADP, $L_N$ ; (2) max. ATP/ADP ratio, $L_T$ ; or (3) inhibition of the phosphorylation pathway, $L_{Omy}$ |
| OXPHOS | $P$ ; high ADP-stimulated respiration       | max.       | high          | Kinetically saturating [ADP] and $[P_i]$                      | $J_{P\gg}$ by phosphorylation pathway; or $J_{O_2,k}$ by ET-pathway capacity  |
| ET     | $E$ ; max. noncoupled respiration           | 0          | low           | Optimal external uncoupler concentration for max. oxygen flux | $J_{O_2,k}$ by ET-pathway capacity  |
| ROX    | $R_{ox}$ ; min. residual $O_2$ consumption  | 0          | 0             | $J_{O_2,Rox}$ in non-ET-pathway oxidation reactions           | Full inhibition of ET-pathway or absence of fuel substrates   |

385  
 386  
 387 **LEAK state (Fig. 3):** The  
 388 LEAK state is defined as a state  
 389 of mitochondrial respiration  
 390 when  $O_2$  flux mainly  
 391 compensates for the proton leak  
 392 in the absence of ATP synthesis,  
 393 at kinetically saturating  
 394 concentrations of  $O_2$  and  
 395 respiratory substrates. LEAK  
 396 respiration is measured to obtain  
 397 an indirect estimate of *intrinsic uncoupling* without addition of any experimental uncoupler: (1)

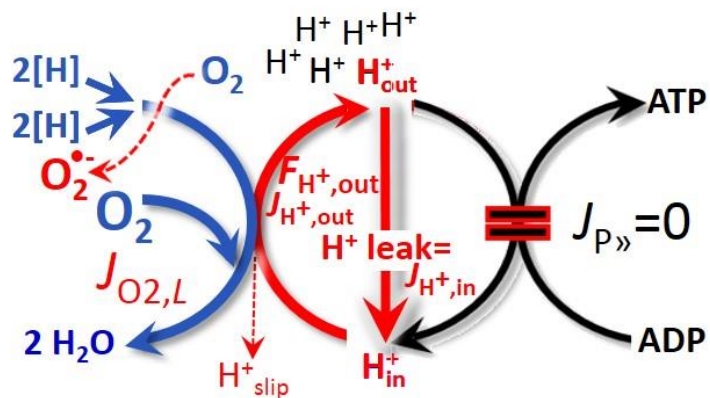


**Fig. 3. LEAK state:** Phosphorylation is arrested,  $J_{P\gg}=0$ , and oxygen flux,  $J_{O_2,L}$ , is controlled mainly by the proton leak, which equals  $J_{H^+,in}$ , at maximum protonmotive force,  $F_{H^+,out}$  (See also Fig. 2).

398 in the absence of adenylates; (2) after depletion of ADP at maximum ATP/ADP ratio; or (3)  
399 after inhibition of the phosphorylation pathway by inhibitors of ATP synthase, such as  
400 oligomycin, or adenine nucleotide translocase, such as carboxyatractyloside.

401 **Proton leak:** Proton leak is the *uncoupled* process in which protons are translocated  
402 across the inner mitochondrial membrane in the dissipative direction of the downhill  
403 protonmotive force without coupling to phosphorylation (**Fig. 3**). The proton leak flux depends  
404 on the protonmotive force, is a property of the inner mitochondrial membrane, may be enhanced  
405 due to possible contaminations by free fatty acids, and is physiologically controlled. In  
406 particular, inducible uncoupling mediated by uncoupling protein 1 (UCP1) is physiologically  
407 controlled, *e.g.*, in brown adipose tissue. UCP1 is a proton channel of the inner mitochondrial  
408 membrane facilitating the conductance of protons across the inner mitochondrial membrane.  
409 As consequence of this effective short-circuit, the protonmotive force diminishes, resulting in  
410 stimulation of electron transfer to oxygen and heat dissipation without phosphorylation of ADP.  
411 Mitochondrial injuries may lead to *dyscoupling* as a pathological or toxicological cause of  
412 *uncoupled* respiration, *e.g.*, as a consequence of opening the permeability transition pore.  
413 Dyscoupled respiration is distinguished from the experimentally induced *noncoupled*  
414 respiration in the ET state. Under physiological conditions, the proton leak is the dominant  
415 contributor to the overall leak current.

416 **Proton slip:** Proton slip is the *decoupled* process in which protons are only partially  
417 translocated by a proton pump of the ET-pathways and slip back to the original compartment  
418 (Dufour *et al.* 1996). Proton slip can also happen in association with the ATP-synthase, in which  
419 case the proton slips downhill across the membrane to the matrix without contributing to ATP  
420 synthesis. In each case, proton slip is a property of the proton pump and increases with the  
421 turnover rate of the pump.

422 **Cation cycling:** Proton leak is a leak current of protons. There can be other cation  
423 contributors to leak current including calcium and probably magnesium. Calcium current is

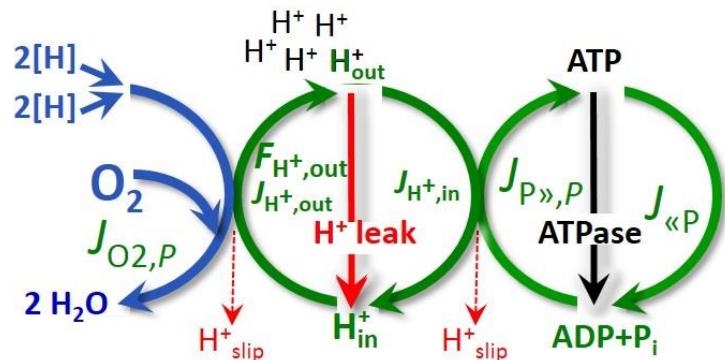


424 balanced by mitochondrial Na/Ca exchange, which is balanced by Na/H exchange or K/H  
 425 exchange. This is another effective uncoupling mechanism different from proton leak and slip.

426 Small differences of terms, *e.g.*, uncoupled, noncoupled, are easily overlooked and may  
 427 be erroneously perceived as identical. Even with an attempt at rigorous definition, the common  
 428 use of such terms may remain vague (**Table 2**).

429 **OXPHOS state (Fig. 4):**

430 The OXPHOS state is defined as  
 431 the respiratory state with  
 432 kinetically saturating  
 433 concentrations of O<sub>2</sub>, respiratory  
 434 and phosphorylation substrates,  
 435 and absence of exogenous  
 436 uncoupler, which provides an  
 437 estimate of the maximal capacity  
 438 of OXPHOS in any given



439 **Fig. 4. OXPHOS state:** Phosphorylation,  $J_{P\gg}$ , is stimulated  
 440 by kinetically saturating [ADP] and inorganic phosphate,  $[P_i]$ ,  
 441 and is supported by a high protonmotive force,  $F_{H^+,out}$ . O<sub>2</sub>  
 442 flux,  $J_{O_2,P}$ , is highly coupled at a maximum  $P\gg/O_2$  ratio,  
 443  $J_{P\gg,P}/J_{O_2,P}$  (See also Fig. 2).

439 pathway control state. Respiratory capacities at kinetically saturating substrate concentrations  
 440 provide reference values or upper limits of performance, aiming at the generation of data sets  
 441 for comparative purposes. Any effects of substrate kinetics are thus separated from reporting  
 442 actual mitochondrial capacity for oxidation during coupled respiration, against which  
 443 physiological activities can be evaluated.

444 As discussed previously, 0.2 mM ADP does not fully saturate flux in isolated  
 445 mitochondria (Gnaiger 2001; Puchowicz *et al.* 2004); greater ADP concentration is required,  
 446 particularly in permeabilized muscle fibres and cardiomyocytes, to overcome limitations by  
 447 intracellular diffusion and by the reduced conductance of the outer mitochondrial membrane  
 448 (Jepihhina *et al.* 2011, Illaste *et al.* 2012, Simson *et al.* 2016) either through interaction with  
 449 tubulin (Rostovtseva *et al.* 2008) or other intracellular structures (Birkedal *et al.* 2014). In

450 permeabilized muscle fibre bundles of high respiratory capacity, the apparent  $K_m$  for ADP  
 451 increases up to 0.5 mM (Saks *et al.* 1998), indicating that >90% saturation is reached only at  
 452 >5 mM ADP. Similar ADP concentrations are also required for accurate determination of  
 453 OXPHOS capacity in human clinical cancer samples and permeabilized cells (ref). Whereas 2.5  
 454 to 5 mM ADP is sufficient to obtain the actual OXPHOS capacity in many types of  
 455 permeabilized cell and tissue preparations, experimental validation is required in each specific  
 456 case.

457

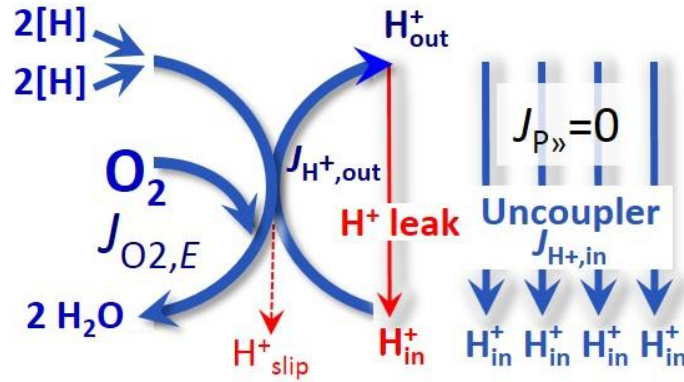
458 **Table 2. Distinction of terms related to coupling.**

| Term                    | Respiration | $P_{\gg}/O_2$ | Note  |
|-------------------------|-------------|---------------|---|
| Fully coupled           | $P - L$     | max.          | OXPHOS capacity corrected for LEAK respiration ( <b>Fig. 6</b> )  |
| Well coupled            | $P$         | high          | Phosphorylating respiration with a variable intrinsic LEAK component ( <b>Fig. 4</b> )                                    |
| Loosely coupled         | up to $E$   | low           | Inducibly uncoupled by UCPI or $Ca^{2+}$ cycling  |
| Dyscoupled              | $P$         | low           | Pathologically, toxicologically, environmentally increased uncoupling, mitochondrial dysfunction                          |
| Uncoupled and decoupled | $L$         | 0             | Non-phosphorylating intrinsic LEAK respiration without added protonophore ( <b>Fig. 3</b> )                               |
| Noncoupled              | $E$         | 0             | Non-phosphorylating respiration stimulated to maximum flux at optimum exogenous uncoupler concentration ( <b>Fig. 5</b> ) |

459

460 **Electron transfer state**

461 (Fig. 5): The ET state is defined  
 462 as the *noncoupled* state with  
 463 kinetically saturating  
 464 concentrations of O<sub>2</sub>, respiratory  
 465 substrate and optimum  
 466 exogenous uncoupler  
 467 concentration for maximum O<sub>2</sub>  
 468 flux, as an estimate of oxidative



469 ET capacity. Inhibition of respiration is observed at higher than optimum uncoupler  
 470 concentrations. As a consequence of the nearly collapsed protonmotive force, the driving force  
 471 is insufficient for phosphorylation and  $J_{P_{\gg}}=0$ .  
**Fig. 5. ET state:** Noncoupled respiration,  $J_{O_2,E}$ , is maximum  
 at optimum exogenous uncoupler concentration and  
 phosphorylation is zero,  $J_{P_{\gg}}=0$  (See also Fig. 2).

469 ET capacity. Inhibition of respiration is observed at higher than optimum uncoupler  
 470 concentrations. As a consequence of the nearly collapsed protonmotive force, the driving force  
 471 is insufficient for phosphorylation and  $J_{P_{\gg}}=0$ .

472 Besides the three fundamental coupling states of mitochondrial preparations, the  
 473 following respiratory state also is relevant to assess respiratory function:

474 **ROX:** Residual oxygen consumption (ROX) is defined as O<sub>2</sub> consumption due to  
 475 oxidative side reactions remaining after inhibition of ET. ROX is not a coupling state but  
 476 represents a baseline that is used to correct mitochondrial respiration in defined coupling states.  
 477 ROX is not necessarily equivalent to non-mitochondrial respiration, considering oxygen-  
 478 consuming reactions in mitochondria not related to ET, such as oxygen consumption in  
 479 reactions catalyzed by monoamine oxidases (type A and B), monooxygenases (cytochrome  
 480 P450 monooxygenases), dioxygenase (sulfur dioxygenase and trimethyllysine dioxygenase),  
 481 several hydroxylases, and more. Mitochondrial preparations, especially those obtained from  
 482 liver, are contaminated by peroxisomes. This fact makes the exact determination of  
 483 mitochondrial oxygen consumption and mitochondria-associated generation of reactive oxygen  
 484 species complicated (Schönfeld *et al.* 2009). The dependence of ROX-linked oxygen  
 485 consumption needs to be studied in detail with respect to non-ET enzyme activities, availability

486 of specific substrates, oxygen concentration, and electron leakage leading to the formation of  
 487 reactive oxygen species.

488

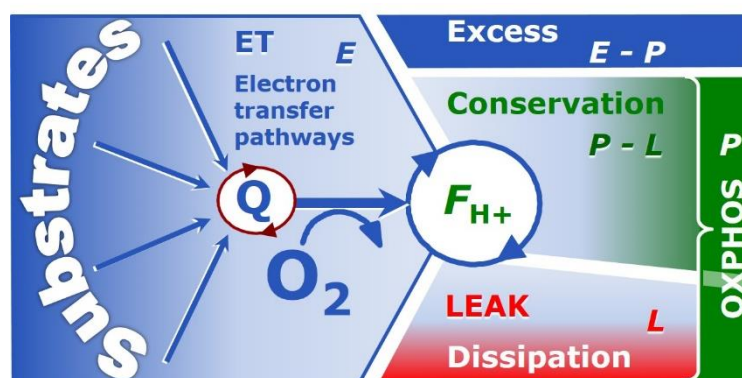
## 489 2.2. Coupling states and respiratory rates

490 It is important to distinguish metabolic pathways from metabolic states and the  
 491 corresponding metabolic rates; for example: electron transfer pathways (**Fig. 6**), ET state (**Fig.**  
 492 **5**), and ET capacity,  $E$ , respectively (**Table 1**). The protonmotive force is *high* in the OXPPOS  
 493 state when it drives phosphorylation, *maximum* in the LEAK state of coupled mitochondria,  
 494 driven by LEAK respiration at a minimum back flux of protons to the matrix side, and *very low*  
 495 in the ET state when uncouplers short-circuit the proton cycle (**Table 1**).

496

497 **Fig. 6. Four-compartment model**  
 498 **of oxidative phosphorylation.**

499 Respiratory states (ET, OXPPOS,  
 500 LEAK) and corresponding rates ( $E$ ,  
 501  $P$ ,  $L$ ) are connected by the  
 502 protonmotive force,  $F_{H+,out}$ . Electron  
 503 transfer capacity,  $E$ , is partitioned



504 into (1) dissipative LEAK respiration,  $L$ , when the capacity to perform work is irreversibly lost, (2) net  
 505 OXPPOS capacity,  $P-L$ , with partial conservation of the capacity to perform work, and (3) the excess  
 506 capacity,  $E-P$ . Modified from Gnaiger (2014).

507

508 The three coupling states, ET, LEAK and OXPPOS, are presented in a schematic context  
 509 with the corresponding respiratory rates, abbreviated as  $E$ ,  $L$  and  $P$ , respectively (**Fig. 6**). This  
 510 clarifies that  $E$  may exceed or be equal to  $P$ , but  $E$  cannot theoretically be lower than  $P$ .  $E < P$   
 511 must be discounted as an artefact, which may be caused experimentally by: (1) loss of oxidative  
 512 capacity during the time course of the respirometric assay, since  $E$  is measured subsequently to  
 513  $P$ ; (2) using too low uncoupler concentrations; (3) using high uncoupler concentrations which

514 inhibit ET (Gnaiger 2008); (4) high oligomycin concentrations applied for measurement of  $L$   
515 before titrations of uncoupler, when oligomycin exerts an inhibitory effect on  $E$ . On the other  
516 hand, the excess ET capacity is overestimated if non-saturating  $[P_i]$  or  $[ADP]$  (State 3) are used.

517  $E > P$  is observed in many types of mitochondria, varying between species, tissues and cell  
518 types. It is the excess ET capacity pushing the phosphorylation pathway flux (**Fig. 1B**) to the  
519 limit of its *capacity of utilizing* the protonmotive force. Within any type of mitochondria, the  
520 magnitude of  $E > P$  depends on (1) the pathway control state with single or multiple electron  
521 input into the Q-junction and involvement of three or fewer coupling sites determining the  
522  $H^+_{out}/O_2$  *coupling stoichiometry* (**Fig. 1A**); and (2) the *biochemical coupling efficiency*  
523 expressed as  $(E-L)/E$ , since an increase of  $L$  causes  $P$  to increase towards the limit of  $E$ . The  
524 *excess E-P capacity*,  $E-P$ , therefore, provides a sensitive diagnostic indicator of specific injuries  
525 of the phosphorylation pathway, under conditions when  $E$  remains constant but  $P$  declines  
526 relative to controls (**Fig. 6**). Substrate cocktails supporting simultaneous convergent electron  
527 transfer to the Q-junction for reconstitution of tricarboxylic acid cycle (TCA cycle) function  
528 establish pathway control states with high ET capacity, and consequently increase the  
529 sensitivity of the  $E-P$  assay.

530 When subtracting  $L$  from  $P$ , the dissipative LEAK component in the OXPHOS state may  
531 be overestimated. This can be avoided by measuring LEAK respiration in a state when the  
532 protonmotive force is adjusted to its slightly lower value in the OXPHOS state, *e.g.*, by titration  
533 of an ET inhibitor. Any turnover-dependent components of proton leak and slip, however, are  
534 underestimated under these conditions (Garlid *et al.* 1993). In general, it is inappropriate to use  
535 the term *ATP production* or *ATP turnover* for the difference of oxygen consumption measured  
536 in states  $P$  and  $L$ . The difference  $P-L$  is the upper limit of the part of OXPHOS capacity that is  
537 freely available for ATP production (corrected for LEAK respiration) and is fully coupled to  
538 phosphorylation with a maximum mechanistic stoichiometry (**Fig. 6**).

539

## 540 2.3. Classical terminology for isolated mitochondria

541 *‘When a code is familiar enough, it ceases appearing like a code; one forgets that*  
 542 *there is a decoding mechanism. The message is identical with its meaning’*  
 543 (Hofstadter 1979).

544 Chance and Williams (1955; 1956) introduced five classical states of mitochondrial respiration  
 545 and cytochrome redox states. **Table 3** shows a protocol with isolated mitochondria in a closed  
 546 respirometric chamber, defining a sequence of respiratory states.

547 **Table 3. Metabolic states of mitochondria (Chance and**  
 548 **Williams, 1956; Table V).**  
 549

| State | [O <sub>2</sub> ] | ADP level | Substrate level | Respiration rate | Rate-limiting substance |
|-------|-------------------|-----------|-----------------|------------------|-------------------------|
| 1     | >0                | low       | low             | slow             | ADP                     |
| 2     | >0                | high      | ~0              | slow             | substrate               |
| 3     | >0                | high      | high            | fast             | respiratory chain       |
| 4     | >0                | low       | high            | slow             | ADP                     |
| 5     | 0                 | high      | high            | 0                | oxygen                  |

550

551 **State 1** is obtained after addition of isolated mitochondria to air-saturated  
 552 isoosmotic/isotonic respiration medium containing inorganic phosphate, but no fuel substrates  
 553 and no adenylates, *i.e.*, AMP, ADP, ATP.

554 **State 2** is induced by addition of a high concentration of ADP (typically 100 to 300  $\mu$ M),  
 555 which stimulates respiration transiently on the basis of endogenous fuel substrates and  
 556 phosphorylates only a small portion of the added ADP. State 2 is then obtained at a low  
 557 respiratory activity limited by zero endogenous fuel substrate availability (**Table 3**). If addition  
 558 of specific inhibitors of respiratory complexes, such as rotenone, does not cause a further  
 559 decline of oxygen consumption, State 2 is equivalent to residual oxygen consumption (See  
 560 below). If inhibition is observed, undefined endogenous fuel substrates are a confounding factor  
 561 of pathway control by externally added substrates and inhibitors. In contrast to the original  
 562 protocol, an alternative sequence of titration steps is frequently applied, in which the alternative

563 State 2 has an entirely different meaning, when this second state is induced by addition of fuel  
564 substrate without ADP (LEAK state; in contrast to State 3 as a ROX state as defined in **Table**  
565 **2**), followed by addition of ADP.

566 **State 3** is the state stimulated by addition of fuel substrates while the ADP concentration  
567 is still high (**Table 3**) and supports coupled energy transformation through oxidative  
568 phosphorylation. 'High ADP' is a concentration of ADP specifically selected to allow the  
569 measurement of State 3 to State 4 transitions of isolated mitochondria in a closed respirometric  
570 chamber. Repeated ADP titration re-establishes State 3 at 'high ADP'. Starting at oxygen  
571 concentrations near air-saturation (ca. 200  $\mu\text{M}$   $\text{O}_2$  at sea level and 37  $^\circ\text{C}$ ), the total ADP  
572 concentration added must be low enough (typically 100 to 300  $\mu\text{M}$ ) to allow phosphorylation  
573 to ATP at a coupled oxygen consumption that does not lead to oxygen depletion during the  
574 transition to State 4. In contrast, kinetically saturating ADP concentrations usually are an order  
575 of magnitude higher than 'high ADP', e.g. 2.5 mM in isolated mitochondria. The abbreviation  
576 State 3u is frequently used in bioenergetics, to indicate the state of respiration after titration of  
577 an uncoupler, without sufficient emphasis on the fundamental difference between OXPHOS  
578 capacity (*well-coupled* with an *endogenous* uncoupled component) and ET capacity  
579 (*noncoupled*).

580 **State 4** is a LEAK state which is obtained only if the mitochondrial preparation is intact  
581 and well-coupled. Depletion of ADP by phosphorylation to ATP leads to a decline in oxygen  
582 consumption in the transition from State 3 to State 4. Under these conditions, a maximum  
583 protonmotive force and high ATP/ADP ratio are maintained, and the  $\text{P}_{\gg}/\text{O}_2$  ratio can be  
584 calculated. State 4 respiration,  $L_T$  (**Table 1**), reflects intrinsic proton leak and intrinsic ATP  
585 hydrolysis activity. Oxygen consumption in State 4 is an overestimation of LEAK respiration  
586 if the contaminating ATP hydrolysis activity recycles some ATP to ADP,  $J_{\ll\text{P}}$ , which stimulates  
587 respiration coupled to phosphorylation,  $J_{\text{P}\gg} > 0$ . This can be tested by inhibition of the  
588 phosphorylation pathway using oligomycin, ensuring that  $J_{\text{P}\gg} = 0$  (State 4o). Alternatively,

589 sequential ADP titrations re-establish State 3, followed by State 3 to State 4 transitions while  
 590 sufficient oxygen is available. However, anoxia may be reached before exhaustion of ADP  
 591 (State 5).

592 **State 5** is the state after exhaustion of oxygen in a closed respirometric chamber.  
 593 Diffusion of oxygen from the surroundings into the aqueous solution may be a confounding  
 594 factor preventing complete anoxia (Gnaiger 2001). Chance and Williams (1955) provide an  
 595 alternative definition of State 5, which gives it the meaning of ROX: ‘State 5 may be obtained  
 596 by antimycin A treatment or by anaerobiosis’.

597 In **Table 3**, only States 3 and 4 (and ‘State 2’ in the alternative protocol without ADP;  
 598 not included in the table) are coupling control states, with the restriction that O<sub>2</sub> flux in State 3  
 599 may be limited kinetically by non-saturating ADP concentrations (**Table 1**).

600

### 601 **3. The protonmotive force and proton flux**

#### 602 *3.1. Electric and chemical partial forces versus electrical and chemical units*

603 The protonmotive force across the inner mitochondrial membrane (Mitchell and Moyle  
 604 1967) was introduced most beautifully in the *Grey Book 1966* (see Mitchell 2011),

$$605 \quad \Delta p_{\text{H}^+} = \Delta \Psi + \Delta \mu_{\text{H}^+}/F \quad (\text{Eq. 1})$$

606 The protonmotive force consists of two partial forces: (1) The electrical part,  $\Delta \Psi$ , is the  
 607 difference of charge (electric potential difference) and is not specific for H<sup>+</sup>. (2) The chemical  
 608 part,  $\Delta \mu_{\text{H}^+}$ , is the chemical potential difference in H<sup>+</sup>, is proportional to the pH difference, and  
 609 incorporates the Faraday constant (**Table 4**).

610

611

612

613

614



615 **Table 4. Protonmotive force and flux matrix.** Rows: Electrical and chemical  
 616 isomorphic format ( $e$  and  $n$ ). The Faraday constant,  $F$ , converts protonmotive force  
 617 and flux from *isomorphic format*  $e$  to  $n$ . Columns: The protonmotive force is the sum of  
 618 *partial isomorphic forces*  $F_{el}$  and  $F_{H+,d}$ . In contrast to force (state), the conjugated flux  
 619 (rate) cannot be partitioned.  
 620

| State                       | Force                     |   | electric              | + chem.               | Unit               | Notes                                |
|-----------------------------|---------------------------|---|-----------------------|-----------------------|--------------------|--------------------------------------|
| Protonmotive force, $e$     | $\Delta p_{H+}$           | = | $\Delta \Psi$         | + $\Delta \mu_{H+}/F$ | $J \cdot C^{-1}$   | $1e$                                 |
| Chemiosmotic potential, $n$ | $\Delta \tilde{\mu}_{H+}$ | = | $\Delta \Psi \cdot F$ | + $\Delta \mu_{H+}$   | $J \cdot mol^{-1}$ | $1n$                                 |
| State                       | Isomorphic force          |   | $F_{H+,out/i}$        | $e_{out}$             | + $H^{+}_{out,d}$  |                                      |
| Electric charge, $e$        | $F_{H+,out/e}$            | = | $F_{el,out/e}$        | + $F_{H+,out,d/e}$    | $J \cdot C^{-1}$   | $2e$                                 |
| Amount of substance, $n$    | $F_{H+,out/n}$            | = | $F_{el,out/n}$        | + $F_{H+,out,d/n}$    | $J \cdot mol^{-1}$ | $2n$                                 |
| Rate                        | Isomorphic flux           |   | $J_{H+,out/i}$        | $e$                   | or $n$             |                                      |
| Electric charge, $e$        | $J_{H+,out/e}$            |   | $J_{H+,out/e}$        |                       |                    | $C \cdot s^{-1} \cdot m^{-3}$ $3e$   |
| Amount of substance, $n$    | $J_{H+,out/n}$            |   |                       |                       | $J_{H+,out/n}$     | $mol \cdot s^{-1} \cdot m^{-3}$ $3n$ |

621  
 622 1: The Faraday constant,  $F$ , is the product of elementary charge ( $e=1.602177 \cdot 10^{-19} \cdot C$ ) and the  
 623 Avogadro (Loschmidt) constant ( $N_A=6.022136 \cdot 10^{23} \cdot mol^{-1}$ ),  $F=eN_A=96,485.3 \text{ C/mol}$ .  $\Delta \tilde{\mu}_{H+}$  is the  
 624 chemiosmotic potential difference.  $1e$  and  $1n$  are the classical representations of  $2e$  and  $2n$ .  
 625 2: The protonmotive force is  $F_{H+,out}$ , expressed either in isomorphic format  $e$  or  $n$ .  $F_{el/e} \equiv \Delta \Psi$  is the partial  
 626 protonmotive force ( $e$ ) acting generally on charged motive molecules (*i.e.* ions that are displaceable  
 627 across the inner mitochondrial membrane). In contrast,  $F_{H+,d/n} \equiv \Delta \mu_{H+}$  is the partial protonmotive force  
 628 specific for proton displacement ( $H^+_d$ ). The sign of the force is negative for exergonic transformations  
 629 in which exergy is lost or dissipated, and positive for endergonic transformations which conserve  
 630 exergy from a coupled exergonic process (**Box 3**).  
 631 3: The sign of the flux depends on the definition of the compartmental direction of the translocation (**Fig.**  
 632 **2**). Flux x force =  $J_{H+,out/e} \cdot F_{H+,out/e} = J_{H+,out/n} \cdot F_{H+,out/n} = \text{Volume-specific power } [J \cdot s^{-1} \cdot m^{-3} = W \cdot m^{-3}]$ .  
 633

634 **Faraday constant**,  $F=eN_A \text{ [C/mol]}$  (**Table 4**), enables the conversion between  
 635 protonmotive force,  $F_{H+,out/e} \equiv \Delta p_{H+} \text{ [J/C]}$ , expressed per *motive charge*,  $e \text{ [C]}$ , and protonmotive  
 636 force or electrochemical potential difference,  $F_{H+,out/n} \equiv \Delta \tilde{\mu}_{H+} = \Delta p_{H+} \cdot F \text{ [J/mol]}$ , expressed per

637 *motive amount of protons*,  $n$  [mol]. Proton charge,  $e$ , and amount of substance,  $n$ , define the  
 638 units for the isomorphic formats. Taken together,  $F$  converts protonmotive force and flux from  
 639 isomorphic format  $e$  to  $n$  (Eq. 2; see also **Table 4**, Note 2),

$$640 \quad F_{\text{H}^+, \text{out}/n} = F_{\text{H}^+, \text{out}/e} \cdot eN_A \quad (\text{Eq. 2.1})$$

$$641 \quad J_{\text{H}^+, \text{out}/n} = J_{\text{H}^+, \text{out}/e} / (eN_A) \quad (\text{Eq. 2.2})$$

642 In each format, the protonmotive force is expressed as the sum of two partial forces. The  
 643 concept expressed by the complex symbols in Eq. 1 can be explained and visualized more easily  
 644 by *partial isomorphic forces* as the components of the protonmotive force:

645 **Electrical part of the protonmotive force:** (1) Isomorph  $e$ :  $F_{\text{el}/e} \equiv \Delta\Psi$  is the electrical  
 646 part of the protonmotive force expressed in units joule per coulomb, *i.e.* volt [V=J/C].  $F_{\text{el}/e}$  is  
 647 defined as partial Gibbs energy change per *motive elementary charge*,  $e$  [C], not specific for  
 648 proton charge (**Table 4**, Note 2e). (2) Isomorph  $n$ :  $F_{\text{el}/n} \equiv \Delta\Psi \cdot F$  is the electric force expressed  
 649 in units joule per mole [J/mol], defined as partial Gibbs energy change per *motive amount of*  
 650 *charge*,  $n$  [mol], not specific for proton charge (**Table 4**, Note 2n).

651 **Chemical part of the protonmotive force:** (1) Isomorph  $n$ :  $F_{\text{d}, \text{H}^+/n} \equiv \Delta\mu_{\text{H}^+}$  is the chemical  
 652 part (diffusion, displacement of  $\text{H}^+$ ) of the protonmotive force expressed in units joule per mole  
 653 [J/mol].  $F_{\text{d}, \text{H}^+/n}$  is defined as partial Gibbs energy change per *motive amount of protons*,  $n$  [mol]  
 654 (**Table 4**, Note 2n). (2) Isomorph  $e$ :  $F_{\text{d}, \text{H}^+/e} \equiv \Delta\mu_{\text{H}^+}/F$  is the chemical force expressed in units  
 655 joule per coulomb [V], defined as partial Gibbs energy change per *motive amount of protons*  
 656 *expressed in units of electric charge*,  $e$  [C], but specific for proton charge (**Table 4**, Note 2e).

657 Protonmotive means that there is a potential for the movement of protons, and force is a  
 658 measure of the potential for motion. Motion is relative and not absolute (Principle of Galilean  
 659 Relativity); likewise there is no absolute potential, but (isomorphic) forces are potential  
 660 differences. An electric partial force expressed in the format of electric charge,  $F_{\text{el}/e}$ , of -0.2 V  
 661 (**Table 5**, Note 5e) is equivalent to force in the format of amount,  $F_{\text{el}, \text{H}^+/n}$ , of  $19 \text{ kJ} \cdot \text{mol}^{-1} \text{ H}^+_{\text{out}}$   
 662 (Note 5n). For a  $\Delta\text{pH}$  of 1 unit, the chemical partial force in the format of amount,  $F_{\text{d}, \text{H}^+/n}$ ,

663 changes by  $5.9 \text{ kJ}\cdot\text{mol}^{-1}$  (**Table 5**, Note 6n) and chemical force in the format of charge  $F_{d,H+/e}$   
664 changes by 0.06 V (Note 6e). Considering a driving force of  $-470 \text{ kJ}\cdot\text{mol}^{-1} \text{ O}_2$  for oxidation, the  
665 thermodynamic limit of the  $\text{H}^+_{\text{out}}/\text{O}_2$  ratio is reached at a value of  $470/19=24$ , compared to a  
666 mechanistic stoichiometry of 20 (**Fig. 1**).

667

### 668 3.2. Definitions

669 **Control and regulation:** The terms metabolic *control* and *regulation* are frequently used  
670 synonymously, but are distinguished in metabolic control analysis: ‘We could understand the  
671 regulation as the mechanism that occurs when a system maintains some variable constant over  
672 time, in spite of fluctuations in external conditions (homeostasis of the internal state). On the  
673 other hand, metabolic control is the power to change the state of the metabolism in response to  
674 an external signal’ (Fell 1997). Respiratory control may be induced by experimental control  
675 signals that *exert* an influence on: (1) ATP demand and ADP phosphorylation rate; (2) fuel  
676 substrate composition, pathway competition; (3) available amounts of substrates and oxygen,  
677 *e.g.*, starvation and hypoxia; (3) the protonmotive force, redox states, flux-force relationships,  
678 coupling and efficiency; (4)  $\text{Ca}^{2+}$  and other ions including  $\text{H}^+$ ; (5) inhibitors, *e.g.*, nitric oxide  
679 or intermediary metabolites, such as oxaloacetate; (6) signalling pathways and regulatory  
680 proteins, *e.g.* insulin resistance, transcription factor HIF-1 or inhibitory factor 1. *Mechanisms*  
681 of respiratory control and regulation include adjustments of (1) enzyme activities by allosteric  
682 mechanisms and phosphorylation, (2) enzyme content, concentrations of cofactors and  
683 conserved moieties (such as adenylates, nicotinamide adenine dinucleotide [ $\text{NAD}^+/\text{NADH}$ ],  
684 coenzyme Q, cytochrome *c*); (3) metabolic channeling by supercomplexes; and (4)  
685 mitochondrial density (enzyme concentrations and membrane area) and morphology (cristae  
686 folding, fission and fusion). (5) Mitochondria are targeted directly by hormones, thereby  
687 affecting their energy metabolism (Lee *et al.* 2013; Gerö and Szabo 2016; Price and Dai 2016;  
688 Moreno *et al.* 2017). Evolutionary or acquired differences in the genetic and epigenetic basis

689 of mitochondrial function (or dysfunction) between subjects and gene therapy; age; gender,  
690 biological sex, and hormone concentrations; life style including exercise and nutrition; and  
691 environmental issues including thermal, atmospheric, toxicological and pharmacological  
692 factors, exert an influence on all control mechanisms listed above (for reviews, see Brown 1992;  
693 Gnaiger 1993a, 2009; 2014; Paradies *et al.* 2014; Morrow *et al.* 2017).

694 **Respiratory control and response:** Lack of control by a metabolic pathway, *e.g.*  
695 phosphorylation pathway, does mean that there will be no response to a variable activating it,  
696 *e.g.* [ADP]. However, the reverse is not true as the absence of a response to [ADP] does not  
697 exclude the phosphorylation pathway from having some degree of control. The degree of  
698 control of a component of the OXPHOS pathway on an output variable, such as oxygen flux,  
699 will in general be different from the degree of control on other outputs, such as phosphorylation  
700 flux or proton leak flux (**Box 2**). As such, it is necessary to be specific as to which input and  
701 output are under consideration (Fell 1997). Therefore, the term respiratory control is elaborated  
702 in more detail in the following section.

703 **Respiratory coupling control:** Respiratory control refers to the ability of mitochondria  
704 to adjust oxygen consumption in response to external control signals by engaging various  
705 mechanisms of control and regulation. Respiratory control is monitored in a mitochondrial  
706 preparation under conditions defined as respiratory states. When phosphorylation of ADP to  
707 ATP is stimulated or depressed, an increase or decrease is observed in electron flux linked to  
708 oxygen consumption in respiratory coupling states of intact mitochondria ('controlled states' in  
709 the classical terminology of bioenergetics). Alternatively, coupling of electron transfer with  
710 phosphorylation is disengaged by disruption of the integrity of the inner mitochondrial  
711 membrane or by uncouplers, functioning like a clutch in a mechanical system. The  
712 corresponding coupling control state is characterized by high levels of oxygen consumption  
713 without control by phosphorylation ('uncontrolled state'). Energetic coupling is defined in **Box**  
714 **4**. Loss of coupling by intrinsic uncoupling and decoupling, or pathological dyscoupling lowers

715 the efficiency. Such generalized uncoupling is different from switching to mitochondrial  
 716 pathways that involve fewer than three proton pumps ('coupling sites': Complexes CI, CIII and  
 717 CIV), bypassing CI through multiple electron entries into the Q-junction (**Fig. 1**). A bypass of  
 718 CIII and CIV is provided by alternative oxidases, which reduce oxygen without proton  
 719 translocation. Reprogramming of mitochondrial pathways may be considered as a switch of  
 720 gears (changing the stoichiometry) rather than uncoupling (loosening the stoichiometry).

721 **Pathway control states** are obtained in mitochondrial preparations by depletion of  
 722 endogenous substrates and addition to the mitochondrial respiration medium of fuel substrates  
 723 (CHNO) and specific inhibitors, activating selected mitochondrial pathways (**Fig. 1**). Coupling  
 724 control states and pathway control states are complementary, since mitochondrial preparations  
 725 depend on an exogenous supply of pathway-specific fuel substrates and oxygen (Gnaiger 2014).

726

---

## 727 **Box 2: Metabolic fluxes and flows: vectorial and scalar**

728 In mitochondrial electron transfer (**Fig. 1**), vectorial transmembrane proton flux is coupled  
 729 through the proton pumps CI, CIII and CIV to the catabolic flux of scalar reactions, collectively  
 730 measured as oxygen flux. In **Fig. 2**, the scalar catabolic reaction,  $k$ , of oxygen consumption,  
 731  $J_{O_2,k}$  [ $\text{mol}\cdot\text{s}^{-1}\cdot\text{m}^{-3}$ ], is expressed as oxygen flux per volume,  $V$  [ $\text{m}^3$ ], of the instrumental chamber  
 732 (the system).

733 Fluxes are *vectors*, if they have *spatial* direction in addition to magnitude. A vector flux  
 734 (surface-density of flow) is expressed per unit cross-sectional area,  $A$  [ $\text{m}^2$ ], perpendicular to the  
 735 direction of flux. If *flows*,  $I$ , are defined as extensive quantities of the *system*, as vector or scalar  
 736 flow,  $I$  or  $I$  [ $\text{mol}\cdot\text{s}^{-1}$ ], respectively, then the corresponding vector and scalar *fluxes*,  $J$ , are  
 737 obtained as  $J=I\cdot A^{-1}$  [ $\text{mol}\cdot\text{s}^{-1}\cdot\text{m}^{-2}$ ] and  $J=I\cdot V^{-1}$  [ $\text{mol}\cdot\text{s}^{-1}\cdot\text{m}^{-3}$ ], respectively, expressing flux as an  
 738 area-specific vector or volume-specific scalar quantity.

739 Vectorial transmembrane proton flux,  $J_{H^+,out}$ , is analyzed in a heterogenous  
 740 compartmental system as a quantity with *directional* but not *spatial* information. Translocation

741 of protons across the inner mitochondrial membrane has a defined direction, either from the  
 742 negative compartment (matrix space; N-phase) to the positive compartment (inter-membrane  
 743 space; P-phase) or *vice versa* (**Fig. 2**). The arrows defining the direction of the translocation  
 744 between the two compartments may point upwards or downwards, right or left, without any  
 745 implication that these are actual directions in space. The ‘upper’ compartment of the P-phase is  
 746 neither above nor below the N-phase in a spatial sense, but can be visualized arbitrarily in a  
 747 figure as the upper compartment (**Fig. 2**). In general, the *compartmental direction* of vectorial  
 748 translocation from the N-phase to the P-phase is defined by assigning the initial and final state  
 749 as *ergodynamic compartments*,  $H^+_{in} \rightarrow H^+_{out}$ , respectively, related to work (erg = work) that  
 750 must be performed to lift the proton from a lower to a higher electrochemical potential or from  
 751 the lower to the higher ergodynamic compartment (Gnaiger 1993b).

752 In direct analogy to *vectorial* translocation, the direction of a *scalar* chemical reaction,  $A$   
 753  $\rightarrow B$ , is defined by assigning substrates and products,  $A$  and  $B$ , as ergodynamic compartments.  
 754  $O_2$  is defined as a substrate in respiratory  $O_2$  consumption, which together with the fuel  
 755 substrates comprises the substrate compartment of the catabolic reaction (**Fig. 2**). Volume-  
 756 specific scalar  $O_2$  flux is coupled (**Box 4**) to vectorial translocation. In order to establish a  
 757 quantitative relation between the coupled fluxes, both  $J_{O_2,k}$  and  $J_{H^+,out}$  must be expressed in  
 758 identical units ( $[mol \cdot s^{-1} \cdot m^{-3}]$  or  $[C \cdot s^{-1} \cdot m^{-3}]$ ), yielding the  $H^+_{out}/O_2$  ratio (**Fig. 1**). The *vectorial*  
 759 proton flux in compartmental translocation has *compartmental direction*, distinguished from a  
 760 *vector* flux with *spatial direction*. Likewise, the corresponding protonmotive force is defined  
 761 as an electrochemical potential *difference* between two compartments, in contrast to a *gradient*  
 762 across the membrane or a vector force with defined spatial direction.

763

---

764 **The steady-state:** Mitochondria represent a thermodynamically open system functioning  
 765 as a biochemical transformation system in non-equilibrium states. State variables (protonmotive  
 766 force; redox states) and metabolic fluxes (*rates*) are measured in defined mitochondrial

767 respiratory *states*. Strictly, steady states can be obtained only in open systems, in which changes  
 768 due to *internal* transformations, *e.g.*, O<sub>2</sub> consumption, are instantaneously compensated for by  
 769 *external* fluxes *e.g.*, O<sub>2</sub> supply, such that oxygen concentration does not change in the system  
 770 (Gnaiger 1993b). Mitochondrial respiratory states monitored in closed systems satisfy the  
 771 criteria of pseudo-steady states for limited periods of time, when changes in the system  
 772 (concentrations of O<sub>2</sub>, fuel substrates, ADP, P<sub>i</sub>, H<sup>+</sup>) do not exert significant effects on metabolic  
 773 fluxes (respiration, phosphorylation). Such pseudo-steady states require respiratory media with  
 774 sufficient buffering capacity and kinetically saturating concentrations of substrates to be  
 775 maintained, and thus depend on the kinetics of the processes under investigation. Proton  
 776 turnover,  $J_{\infty H^+}$ , and ATP turnover,  $J_{\infty P}$ , proceed in the steady-state at constant  $F_{H^+,out}$ , when  $J_{\infty H^+}$   
 777  $= J_{H^+,out} = J_{H^+,in}$ , and at constant  $F_{P\gg}$ , when  $J_{\infty P} = J_{P\gg} = J_{\ll P}$  (**Fig. 2**).

778

---

### 779 **Box 3: Endergonic and exergonic transformations, exergy and dissipation**

780 A chemical reaction, or any transformation, is exergonic if the Gibbs energy change (exergy)  
 781 of the reaction is negative at constant temperature and pressure. The sum of Gibbs energy  
 782 changes of all internal transformations in a system can only be negative, *i.e.* exergy is  
 783 irreversibly dissipated. Endergonic reactions are characterized by positive Gibbs energies of  
 784 reaction and cannot proceed spontaneously in the forward direction as defined. For instance,  
 785 the endergonic reaction P $\gg$  is coupled to exergonic catabolic reactions, such that the total Gibbs  
 786 energy change is negative, *i.e.* exergy must be dissipated for the reaction to proceed (**Fig. 2**).

787 In contrast, energy cannot be lost or produced in any internal process, which is the key  
 788 message of the first law of thermodynamics. Thus mitochondria are the sites of energy  
 789 transformation but not energy production. Open and closed systems can gain energy and exergy  
 790 only by external fluxes, *i.e.* uptake from the environment. Exergy is the potential to perform  
 791 work. In the framework of flux-force relationships (**Box 4**), the *partial* derivative of Gibbs  
 792 energy per advancement of a transformation is an isomorphic force,  $F_{tr}$  (**Table 5**, Note 2). In

793 other words, force is equal to exergy/motive unit (in integral form, this definition takes care of  
 794 non-isothermal processes). This formal generalization represents an appreciation of the  
 795 conceptual beauty of Peter Mitchell's innovation of the protonmotive force against the  
 796 background of the established paradigm of the electromotive force (emf) defined at the limit of  
 797 zero current (Cohen *et al.* 2008).

798

799

800 **Table 5. Power, exergy, force, flux, and advancement.**

801

| Expression                  | Symbol             | Definition  | Unit                              | Notes |
|-----------------------------|--------------------|---|-----------------------------------|-------|
| Power, volume-specific      | $P_{V,tr}$         | $P_{V,tr} = J_{tr} \cdot F_{tr} = \partial_{tr}G \cdot \partial t^{-1}$ | $W = J \cdot s^{-1} \cdot m^{-3}$ | 1     |
| Force, isomorphic           | $F_{tr}$           | $F_{tr} = \partial_{tr}G \cdot \partial_{tr}\xi^{-1}$                   | $J \cdot x^{-1}$                  | 2     |
| Flux, isomorphic            | $J_{tr}$           | $J_{tr} = d_{tr}\xi \cdot dt^{-1} \cdot V^{-1}$                         | $x \cdot s^{-1} \cdot m^{-3}$     | 3     |
| Advancement, $n$            | $d_{tr}\xi_{H+/n}$ | $d_{tr}\xi_{H+/n} = d_{tr}n_{H+} \cdot \nu_{H+}^{-1}$                   | Mol                               | $4n$  |
| Advancement, $e$            | $d_{tr}\xi_{H+/e}$ | $d_{tr}\xi_{H+/e} = d_{tr}e_{H+} \cdot \nu_{H+}^{-1}$                   | C                                 | $4e$  |
| Electric partial force, $e$ | $F_{el/e}$         | $F_{el/e} \equiv \Delta\Psi$  | V                                 | $5e$  |
| Electric partial force, $n$ | $F_{el/n}$         | $\Delta\Psi \cdot F = 96.5 \cdot \Delta\Psi$                            | $kJ \cdot mol^{-1}$               | $5n$  |
| Chemical partial force, $e$ | $F_{d,H+/e}$       | $\Delta\mu_{H+}/F = -$<br>$\ln(10) \cdot RT/F \cdot \Delta pH$          | V                                 | $6e$  |
| at 37 °C                    |                    | $= -0.06 \cdot \Delta pH$   | $J \cdot C^{-1}$                  |       |
| Chemical partial force, $n$ | $F_{d,H+/n}$       | $\Delta\mu_{H+} = -\ln(10) \cdot RT \cdot \Delta pH$                    | $J \cdot mol^{-1}$                | $6n$  |
| at 37 °C                    |                    | $= -5.9 \cdot \Delta pH$  | $kJ \cdot mol^{-1}$               |       |

802

803 1 to 4: An isomorphic motive entity or transformant, expressed in units  $x$ , is defined for any804 transformation, tr.  $x = \text{mol}$  or C in proton translocation.805 2:  $\partial_{tr}G$  [J] is the partial Gibbs energy change in the advancement of transformation tr.806 3: For  $x = \text{C}$ , flow is electric current,  $I_{el}$  [ $A = C \cdot s^{-1}$ ], vector flux is electric current density per area,  $J_{el}$ ,  
807 and compartmental flux is electric current density per volume,  $j_{el}$  [ $A \cdot m^{-3}$ ].808  $4n$ : For a chemical reaction, the advancement of reaction  $r$  is  $d_r\xi_B = d_r n_B \cdot \nu_B^{-1}$  [mol]. The stoichiometric809 number is  $\nu_B = -1$  or  $\nu_B = 1$ , depending on B being a product or substrate, respectively, in reaction  $r$ 810 involving one mole of B. The conjugated *intensive* molar quantity,  $F_{B,r} = \partial_r G / \partial_r \xi_B$  [ $J \cdot mol^{-1}$ ], is the



811 chemical force of reaction or *reaction-motive* force per stoichiometric amount of B. In reaction  
 812 kinetics,  $d_r n_B$  is expressed as a volume-specific quantity, which is the partial contribution to the  
 813 total concentration change of B,  $d_r c_B = d_r n_B / V$  and  $d_c c_B = d_c n_B / V$ , respectively. In open systems with  
 814 constant volume  $V$ ,  $d c_B = d_r c_B + d_e c_B$ , where  $r$  indicates the *internal* reaction and  $e$  indicates the  
 815 *external* flux of B into the unit volume of the system. At steady state the concentration does not  
 816 change,  $d c_B = 0$ , when  $d_r c_B$  is compensated for by the external flux of B,  $d_r c_B = -d_e c_B$  (Gnaiger  
 817 1993b). Alternatively,  $d c_B = 0$  when B is held constant by different coupled reactions in which B  
 818 acts as a substrate or a product.

819 4e: Scalar potential difference across the mitochondrial membrane. In a scalar electric transformation  
 820 (flux of charge, *i.e.* volume-specific current, from the matrix space to the intermembrane and  
 821 extramitochondrial space) the motive force is the difference of charge (**Box 2**). The endergonic  
 822 direction of translocation is defined in **Fig. 2** as  $H^{+}_{in} \rightarrow H^{+}_{out}$ .

823 5n:  $F = 96.5 \text{ (kJ}\cdot\text{mol}^{-1})/V$ .

824 6: The electric partial force is independent of temperature (Note 5), but the chemical partial force  
 825 depends on absolute temperature,  $T$  [K].

826 6e:  $RT$  is the gas constant times absolute temperature.  $\ln(10) \cdot RT / F = 59.16$  and  $61.54$  mV at 298.15  
 827 and 310.15 K (25 and 37 °C), respectively.

828 6n:  $\ln(10) \cdot RT = 5.708$  and  $5.938 \text{ kJ}\cdot\text{mol}^{-1}$  at 298.15 and 310.15 K (25 and 37 °C), respectively.

829

### 830 3.3. Forces and fluxes in physics and irreversible thermodynamics

831 According to its definition in physics, a potential difference and as such the  
 832 *protonmotive force*,  $\Delta p_{H^+}$ , is not a force *per se* (Cohen *et al.* 2008). The fundamental forces of  
 833 physics are distinguished from *motive forces* of statistical and irreversible thermodynamics.  
 834 Complementary to the attempt towards unification of fundamental forces defined in physics,  
 835 the concepts of Nobel laureates Lars Onsager, Erwin Schrödinger, Ilya Prigogine and Peter  
 836 Mitchell (even if expressed in apparently unrelated terms) unite the diversity of *generalized* or  
 837 ‘isomorphic’ *flux-force* relationships, the product of which links to the dissipation function and  
 838 Second Law of thermodynamics (Schrödinger 1944; Prigogine 1967). A *motive force* is the  
 839 derivative of potentially available or ‘free’ energy (exergy) per isomorphic *motive* unit (**Box 3**).

840 Perhaps the first account of a *motive force* in energy transformation can be traced back to the  
841 Peripatetic school around 300 BC in the context of moving a lever, up to Newton's motive force  
842 proportional to the alteration of motion (Coopersmith 2010).

843       **Vectorial and scalar forces, and fluxes:** In chemical reactions and osmotic or diffusion  
844 processes occurring in a closed heterogeneous system, such as a chamber containing isolated  
845 mitochondria, scalar transformations occur without measured spatial direction but between  
846 separate compartments (translocation between the matrix and intermembrane space) or between  
847 energetically-separated chemical substances (reactions from substrates to products). Hence, the  
848 corresponding fluxes are not vectorial but scalar, and are expressed per volume and not per  
849 membrane area (**Box 2**). The corresponding motive forces are also scalar potential *differences*  
850 across the membrane (**Table 5**), without taking into account the *gradients* across the 6 nm thick  
851 inner mitochondrial membrane (Rich 2003).

852       **Coupling:** In energetics (ergodynamics), coupling is defined as an exergy transformation  
853 fuelled by an exergonic (downhill) input process driving the advancement of an endergonic  
854 (uphill) output process. The (negative) output/input power ratio is the efficiency of a coupled  
855 energy transformation (**Box 4**). At the limit of maximum efficiency of a completely coupled  
856 system, the (negative) input power equals the (positive) output power, such that the total power  
857 approaches zero at the maximum efficiency of 1, and the process becomes fully reversible  
858 without any dissipation of exergy, *i.e.* without entropy production.

859

---

860 **Box 4: Coupling, power and efficiency, at constant temperature and pressure**

861 Energetic coupling means that two processes of energy transformation are linked such that the  
862 input power,  $P_{in}$ , is the driving element of the output power,  $P_{out}$ , and the out/input power ratio  
863 is the efficiency. In general, power is work per unit time [ $J \cdot s^{-1} = W$ ]. When describing a system  
864 with volume  $V$  without information on the internal structure, the output is defined as the *external*  
865 work (exergy) performed by the *total* system on its environment. Such a system may be open

866 for any type of exchange, or closed and thus allowing only heat and work to be exchanged  
 867 across the system boundaries. This is the classical black box approach of thermodynamics. In  
 868 contrast, in a colourful compartmental analysis of *internal* energy transformations (**Fig. 2**), the  
 869 system is structured and described by definition of ergodynamic compartments (with  
 870 information on the heterogeneity of the system; **Box 2**) and analysis of separate parts, *i.e.* a  
 871 sequence of *partial* energy transformations, tr. In general, power per unit volume,  $P_{tr}/V$  [W.L<sup>-1</sup>],  
 872 is the product of a volume-specific flux,  $J_{tr}$ , and its conjugated force,  $F_{tr}$ , and is closely linked  
 873 to the dissipation function using the terminology of irreversible thermodynamics (Prigogine  
 874 1967; Gnaiger 1993a,b). Output power of proton translocation and catabolic input power are  
 875 (**Fig. 2**),

876 Output: 
$$P_{H^+,out}/V = J_{H^+,out} \cdot F_{H^+,out}$$

877 Input: 
$$P_k/V = J_{O_2,k} \cdot F_{O_2,k}$$

878  $F_{O_2,k}$  is the exergonic input force with a negative sign, and,  $F_{H^+,out}$ , is the endergonic output  
 879 force with a positive sign (**Box 3**). Ergodynamic efficiency is the ratio of output/input power,  
 880 or the flux ratio times force ratio (Gnaiger 1993a,b),

881 
$$\varepsilon = \frac{P_{H^+,out}}{-P_k} = \frac{J_{H^+,out}}{J_{O_2,k}} \cdot \frac{F_{H^+,out}}{-F_{O_2,k}}$$

882 The concept of incomplete coupling relates exclusively to the first term, *i.e.* the flux ratio, or  
 883  $H^+_{out}/O_2$  ratio (**Fig. 1**). Likewise, respirometric definitions of the P $\gg$ /O<sub>2</sub> ratio and biochemical  
 884 coupling efficiency (Section 3.2) consider flux ratios. In a completely coupled process, the  
 885 power efficiency,  $\varepsilon$ , depends entirely on the force ratio, ranging from zero efficiency at an  
 886 output force of zero, to the limiting output force and maximum efficiency of 1.0, when the total  
 887 power of the coupled process,  $P_{tr}=P_k+P_{H^+,out}$ , equals zero, and any net flows are zero at  
 888 ergodynamic equilibrium of a coupled process. Thermodynamic equilibrium is defined as the  
 889 state when all potentials (all forces) are dissipated and equilibrate towards their minima of zero.  
 890 In a fully or completely coupled process, output and input fluxes are directly proportional in a

891 fixed ratio technically defined as a stoichiometric relationship (a gear ratio in a mechanical  
892 system). Such maximal stoichiometric output/input flux ratios are considered in OXPHOS  
893 analysis as the upper limits or mechanistic  $H^+_{out}/O_2$  and  $P_{\gg}/O_2$  ratios (**Fig. 1**).

---

894  
895 **Coupled versus bound processes:** Since the chemiosmotic theory describes the  
896 mechanisms of coupling in OXPHOS, it may be interesting to ask if the electrical and chemical  
897 parts of proton translocation are coupled processes. This is not the case according to the  
898 definition of coupling. If the coupling mechanism is disengaged, the output process becomes  
899 independent of the input process, and both proceed in their downhill (exergonic) direction (**Fig.**  
900 **2**). It is not possible to physically uncouple the electrical and chemical processes, which are  
901 only *theoretically* partitioned as electrical and chemical components and can be measured  
902 separately. If partial processes are non-separable, *i.e.*, cannot be uncoupled, then these are not  
903 *coupled* but are defined as *bound* processes. The electrical and chemical parts are tightly bound  
904 partial forces of the protonmotive force, since a flux cannot be partitioned but expressed only  
905 in either an electrical or chemical isomorphic format (**Table 4**).

906

#### 907 **4. Normalization: fluxes and flows**

908 The challenges of measuring mitochondrial respiratory flux are matched by those of  
909 normalization, whereby  $O_2$  consumption may be considered as the nominator and normalization  
910 as the complementary denominator, which are tightly linked in reporting the measurements in  
911 a format commensurate with the requirements of a database.

912

##### 913 *4.1. Flux per chamber volume*

914 When the reactor volume does not change during the reaction, which is typical for liquid  
915 phase reactions, the volume-specific *flux of a chemical reaction*  $r$  is the time derivative of the  
916 advancement of the reaction per unit volume,  $J_{V,B} = d_r \zeta_B / dt \cdot V^{-1}$  [(mol·s<sup>-1</sup>)·L<sup>-1</sup>]. The *rate of*

917 *concentration change* is  $dc_B/dt$  [ $(\text{mol}\cdot\text{L}^{-1})\cdot\text{s}^{-1}$ ], where concentration is  $c_B=n_B/V$ . It is helpful to  
 918 make the subtle distinction between  $[\text{mol}\cdot\text{s}^{-1}\cdot\text{L}^{-1}]$  and  $[\text{mol}\cdot\text{L}^{-1}\cdot\text{s}^{-1}]$  for the fundamentally  
 919 different quantities of volume-specific flux and rate of concentration change, which merge to a  
 920 single expression only in closed systems. In open systems, external fluxes (such as  $\text{O}_2$  supply)  
 921 are distinguished from internal transformations (metabolic flux,  $\text{O}_2$  consumption). In a closed  
 922 system, external flows of all substances are zero and  $\text{O}_2$  consumption (internal flow),  $I_{\text{O}_2}$   
 923 [ $\text{pmol}\cdot\text{s}^{-1}$ ], causes a decline of the amount of  $\text{O}_2$  in the system,  $n_{\text{O}_2}$  [ $\text{nmol}$ ]. Normalization of  
 924 these quantities for the volume of the system,  $V$  [ $\text{L}=\text{dm}^3$ ], yields volume-specific  $\text{O}_2$  flux,  
 925  $J_{V,\text{O}_2}=I_{\text{O}_2}/V$  [ $\text{nmol}\cdot\text{s}^{-1}\cdot\text{L}^{-1}$ ], and  $\text{O}_2$  concentration,  $[\text{O}_2]$  or  $c_{\text{O}_2}=n_{\text{O}_2}/V$  [ $\text{nmol}\cdot\text{mL}^{-1}=\mu\text{mol}\cdot\text{L}^{-1}=\mu\text{M}$ ].  
 926 Instrumental background  $\text{O}_2$  flux is due to external flux into a non-ideal closed respirometer,  
 927 such that total volume-specific flux has to be corrected for instrumental background  $\text{O}_2$  flux,  
 928 *i.e.*  $\text{O}_2$  diffusion into or out of the instrumental chamber.  $J_{V,\text{O}_2}$  is relevant mainly for  
 929 methodological reasons and should be compared with the accuracy of instrumental resolution  
 930 of background-corrected flux, *e.g.*  $\pm 1 \text{ nmol}\cdot\text{s}^{-1}\cdot\text{L}^{-1}$  (Gnaiger 2001). ‘Metabolic’ or catabolic  
 931 indicates  $\text{O}_2$  flux,  $J_{\text{O}_2,k}$ , corrected for instrumental background  $\text{O}_2$  flux and chemical background  
 932  $\text{O}_2$  flux due to autoxidation of chemical components added to the incubation medium.

933

#### 934 4.2. System-specific and sample-specific normalization

935 Application of common and generally defined units is required for direct transfer of  
 936 reported results into a database. The second [s] is the *SI* unit for the base quantity *time*. It is also  
 937 the standard time-unit used in solution chemical kinetics. **Table 6** lists some conversion factors  
 938 to obtain *SI* units. The term *rate* is not sufficiently defined to be useful for a database (**Fig. 7**).  
 939 The inconsistency of the meanings of rate becomes fully apparent when considering Galileo  
 940 Galilei’s famous principle, that ‘bodies of different weight all fall at the same rate (have a  
 941 constant acceleration)’ (Coopersmith 2010).

942 **Extensive quantities:** An extensive quantity increases proportionally with system size.  
 943 The magnitude of an extensive quantity is completely additive for non-interacting subsystems,  
 944 such as mass or flow expressed per defined system. The magnitude of these quantities depends  
 945 on the extent or size of the system (Cohen *et al.* 2008).

946

947 **Fig. 7. Different meanings of rate**948 **may lead to confusion, if the**949 **normalization is not sufficiently**950 **specified.** Results are frequently951 expressed as mass-specific flux,  $J_m$ ,

952 per mg protein, dry or wet weight

953 (mass). Cell volume,  $V_{\text{cell}}$ , or954 mitochondrial volume,  $V_{\text{mt}}$ , may be

955 used for normalization (volume-

956 specific flux,  $J_{V_{\text{cell}}}$  or  $J_{V_{\text{mt}}}$ ), which then must be clearly distinguished from flux,  $J_v$ , expressed for957 methodological reasons per volume of the measurement system, or flow per cell,  $I_x$ .

958

959 **Size-specific quantities:** ‘The adjective *specific* before the name of an extensive quantity960 is often used to mean *divided by mass*’ (Cohen *et al.* 2008). Mass-specific flux is flow divided

961 by mass of the system. A mass-specific quantity is independent of the extent of non-interacting

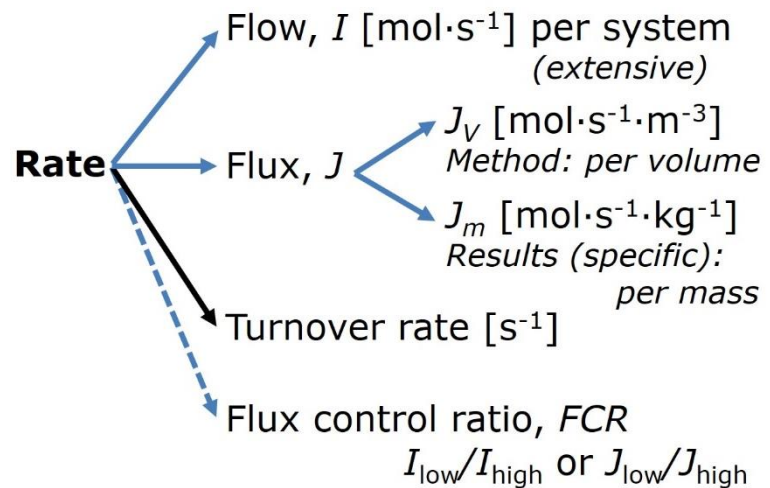
962 homogenous subsystems. Tissue-specific quantities are of fundamental interest in comparative

963 mitochondrial physiology, where *specific* refers to the *type* rather than *mass* of the tissue. The964 term *specific*, therefore, must be further clarified, such that tissue mass-specific, *e.g.*, muscle

965 mass-specific quantities are defined.

966 **Molar quantities:** ‘The adjective *molar* before the name of an extensive quantity967 generally means *divided by amount of substance*’ (Cohen *et al.* 2008). The notion that all molar968 quantities then become *intensive* causes ambiguity in the meaning of *molar Gibbs energy*. It is

969 important to emphasize the fundamental difference between normalization for amount of



959 **Size-specific quantities:** ‘The adjective *specific* before the name of an extensive quantity  
 960 is often used to mean *divided by mass*’ (Cohen *et al.* 2008). Mass-specific flux is flow divided  
 961 by mass of the system. A mass-specific quantity is independent of the extent of non-interacting  
 962 homogenous subsystems. Tissue-specific quantities are of fundamental interest in comparative  
 963 mitochondrial physiology, where *specific* refers to the *type* rather than *mass* of the tissue. The  
 964 term *specific*, therefore, must be further clarified, such that tissue mass-specific, *e.g.*, muscle  
 965 mass-specific quantities are defined.

966 **Molar quantities:** ‘The adjective *molar* before the name of an extensive quantity  
 967 generally means *divided by amount of substance*’ (Cohen *et al.* 2008). The notion that all molar  
 968 quantities then become *intensive* causes ambiguity in the meaning of *molar Gibbs energy*. It is  
 969 important to emphasize the fundamental difference between normalization for amount of

970 substance *in a system* or for amount of motive substance *in a transformation*. When the Gibbs  
 971 energy of a system,  $G$  [J], is divided by the amount of substance B in the system,  $n_B$  [mol], a  
 972 *size-specific* molar quantity is obtained,  $G_B = G/n_B$  [J·mol<sup>-1</sup>], which is not any force at all. In  
 973 contrast, when the partial Gibbs energy change,  $\partial_r G$  [J], is divided by the motive amount of  
 974 substance B in reaction  $r$  (advancement of reaction),  $\partial_r \zeta_B$  [mol], the resulting intensive molar  
 975 quantity,  $F_{r,B} = \partial G / \partial_r \zeta_B$  [J·mol<sup>-1</sup>], is the chemical motive force of reaction  $r$  involving 1 mol B  
 976 (**Table 5**, Note 4).

977 **Flow per system,  $I$ :** In analogy to electrical terms, flow as an extensive quantity ( $I$ ; per  
 978 system) is distinguished from flux as a size-specific quantity ( $J$ ; per system size) (**Fig. 7**).  
 979 Electric current is flow,  $I_{el}$  [A=C·s<sup>-1</sup>] per system (extensive quantity). When dividing this  
 980 extensive quantity by system size (membrane area), a size-specific quantity is obtained, which  
 981 is electric flux (electric current density),  $J_{el}$  [A·m<sup>-2</sup> = C·s<sup>-1</sup>·m<sup>-2</sup>].

982 **Size-specific flux,  $J$ :** Metabolic O<sub>2</sub> flow per tissue increases as tissue mass is increased.  
 983 Tissue mass-specific O<sub>2</sub> flux should be independent of the size of the tissue sample studied in  
 984 the instrument chamber, but volume-specific O<sub>2</sub> flux (per volume of the instrument chamber,  
 985  $V$ ) should increase in direct proportion to the amount of sample in the chamber. Accurate  
 986 definition of the experimental system is decisive: whether the experimental chamber is the  
 987 closed, open, isothermal or non-isothermal *system* with defined volume as part of the  
 988 measurement apparatus, in contrast to the experimental *sample* in the chamber (**Table 6**).  
 989 Volume-specific O<sub>2</sub> flux depends on mass-concentration of the sample in the chamber, but  
 990 should be independent of the chamber volume. There are practical limitations to increasing the  
 991 mass-concentration of the sample in the chamber, when one is concerned about crowding  
 992 effects and instrumental time resolution.

993 **Sample concentration  $C_{mX}$ :** Normalization for sample concentration is required for  
 994 reporting respiratory data. Consider a tissue or cells as the sample,  $X$ , and the sample mass,  $m_X$   
 995 [mg] from which a mitochondrial preparation is obtained. The sample mass is frequently

996 measured as wet or dry weight ( $m_X \equiv W_w$  or  $W_d$  [mg]), or as amount of tissue or cell protein  
 997 ( $m_X \equiv m_{\text{Protein}}$ ). In the case of permeabilized tissues, cells, and homogenates, the sample  
 998 concentration,  $C_{mX} = m_X/V$  [ $\text{mg} \cdot \text{mL}^{-1} = \text{g} \cdot \text{L}^{-1}$ ], is simply the mass of the subsample of tissue that is  
 999 transferred into the instrument chamber. Part of the mitochondria from the tissue is lost during  
 1000 preparation of isolated mitochondria, and only a fraction of mitochondria is obtained, expressed  
 1001 as the mitochondrial yield (**Fig. 8**). At a high mitochondrial yield the sample of isolated  
 1002 mitochondria is more representative of the total mitochondrial population than in preparations  
 1003 characterized by low mitochondrial yield. Determination of the mitochondrial yield is based on  
 1004 measurement of the concentration of a mitochondrial marker in the tissue homogenate,  $C_{\text{mte,thom}}$ ,  
 1005 which simultaneously provides information on the specific mitochondrial density in the sample  
 1006 (**Fig. 8**).

1007 Tissues can contain multiple cell populations which may have distinct mitochondrial  
 1008 subtypes. Mitochondria are also in a constant state of flux due to highly dynamic fission and  
 1009 fusion cycles, and can exist in multiple stages and sizes which may be altered by a range of  
 1010 factors. The isolation of mitochondria (often achieved through differential centrifugation) can  
 1011 therefore yield a subsample of the mitochondrial types present in a tissue, dependent on  
 1012 isolation protocols utilized (*e.g.* centrifugation speed). This possible artefact should be taken  
 1013 into account when planning experiments using isolated mitochondria. The tendency for  
 1014 mitochondria of specific sizes to be enriched at different centrifugation speeds also has the  
 1015 potential to allow the isolation of specific mitochondrial subpopulations and therefore the  
 1016 analysis of mitochondria from multiple cell lineages within a single tissue.

1017 **Mass-specific flux,  $J_{mX,O_2}$ :** Mass-specific flux is obtained by expressing respiration per  
 1018 mass of sample,  $m_X$  [mg].  $X$  is the type of sample, *e.g.*, tissue homogenate, permeabilized fibres  
 1019 or cells. Volume-specific flux is divided by mass concentration of  $X$ ,  $J_{mX,O_2} = J_{V,O_2}/C_{mX}$ ; or flow  
 1020 per cell is divided by mass per cell,  $J_{m\text{cell},O_2} = I_{\text{cell},O_2}/M_{\text{cell}}$ . If mass-specific  $O_2$  flux is constant  
 1021 and independent of sample size (expressed as mass), then there is no interaction between the



1022 subsystems. A 1.5 mg and a 3.0 mg muscle sample respire at identical mass-specific flux.  
 1023 Mass-specific O<sub>2</sub> flux, however, may change with the mass of a tissue sample, cells or isolated  
 1024 mitochondria in the measuring chamber, in which case the nature of the interaction becomes an  
 1025 issue. Optimization of cell density and arrangement is generally important and particularly in  
 1026 experiments carried out in wells, considering the confluency of the cell monolayer or clumps  
 1027 of cells (Salabei *et al.* 2014).

1028

1030 **Table 6. Sample concentrations and normalization of flux with SI/ base units.**

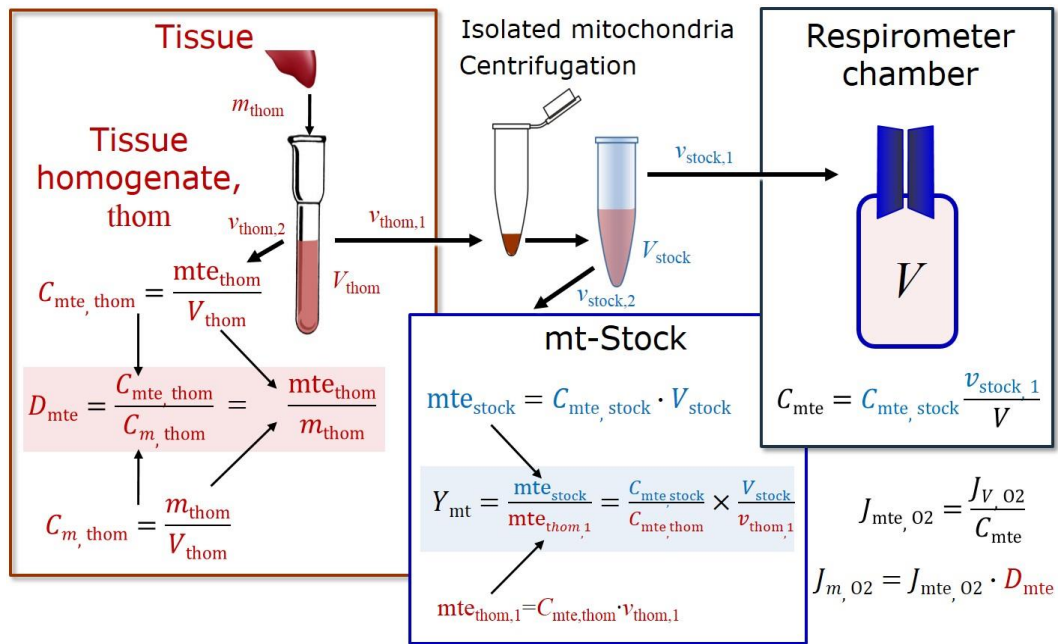
| Expression                                   | Symbol           | Definition                                   | SI Unit   | Notes |
|--|------------------|--|---|-------|
| <b>Sample</b>                                |                  |  |   |       |
| Identity of sample                           | $X$              | Cells, animals, patients                     |   |       |
| Number of sample entities $X$                | $N_X$            | Number of cells, <i>etc.</i>                 | x   |       |
| Mass of sample $X$                           | $m_X$            |  | kg  | 1     |
| Mass of entity $X$                           | $M_X$            | $M_X = m_X \cdot N_X^{-1}$                   | kg·x <sup>-1</sup>                                  | 1     |
| <b>Mitochondria</b>                          |                  |  |   |       |
| Mitochondria                                 | mt               | $X=mt$                                       |   |       |
| Amount of mt-elements                        | mte              | Quantity of mt-marker                        | x <sub>mte</sub>                                    |       |
| <b>Concentrations</b>                        |                  |  |   |       |
| Sample number concentration                  | $C_{NX}$         | $C_{NX} = N_X \cdot V^{-1}$                  | x·m <sup>-3</sup>                                   | 2     |
| Sample mass concentration                    | $C_{mX}$         | $C_{mX} = m_X \cdot V^{-1}$                  | kg·m <sup>-3</sup>                                  |       |
| Mitochondrial concentration                  | $C_{mte}$        | $C_{mte} = mte \cdot V^{-1}$                 | x <sub>mte</sub> ·m <sup>-3</sup>                   | 3     |
| Specific mitochondrial density               | $D_{mte}$        | $D_{mte} = mte \cdot m_X^{-1}$               | x <sub>mte</sub> ·kg <sup>-1</sup>                  | 4     |
| Mitochondrial content,<br>mte per entity $X$ | mte <sub>X</sub> | $mte_X = mte \cdot N_X^{-1}$                 | x <sub>mte</sub> ·x <sup>-1</sup>                   | 5     |
| <b>O<sub>2</sub> flow and flux</b>           |                  |  |   |       |
| Flow   | $I_{O_2}$        | Internal flow                                | mol·s <sup>-1</sup>                                 | 6     |
| Volume-specific flux                         | $J_{V,O_2}$      | $J_{V,O_2} = I_{O_2} \cdot V^{-1}$           | mol·s <sup>-1</sup> ·m <sup>-3</sup>                | 7     |
| Flow per sample entity $X$                   | $I_{X,O_2}$      | $I_{X,O_2} = J_{V,O_2} \cdot C_{NX}^{-1}$    | mol·s <sup>-1</sup> ·x <sup>-1</sup>                | 8     |
| Mass-specific flux                           | $J_{mX,O_2}$     | $J_{mX,O_2} = J_{V,O_2} \cdot C_{mX}^{-1}$   | mol·s <sup>-1</sup> ·kg <sup>-1</sup>               | 9     |
| Mitochondria-specific flux                   | $J_{mte,O_2}$    | $J_{mte,O_2} = J_{V,O_2} \cdot C_{mte}^{-1}$ | mol·s <sup>-1</sup> ·x <sub>mte</sub> <sup>-1</sup> | 10    |

1031

1032 1 The SI prefix k is used for the SI base unit of mass (kg=1,000 g). In praxis, various SI prefixes are  
 1033 used for convenience, to make numbers easily readable, e.g. 1 mg tissue, cell or mitochondrial mass  
 1034 instead of 0.000001 kg.

1035 2 In case  $X=cells$ , the sample number concentration is  $C_{Ncell}=N_{cell} \cdot V^{-1}$ , and volume may be expressed  
 1036 in [dm<sup>3</sup>=L] or [cm<sup>3</sup>=mL]. See **Table 7** for different sample types.

- 1037 3 mt-concentration is an experimental variable, dependent on sample concentration: (1)  $C_{mte} = mte \cdot V^{-1}$ ;
- 1038 (2)  $C_{mte} = mte_X \cdot C_{NX}$ ; (3)  $C_{mte} = C_{mX} \cdot D_{mte}$ .
- 1039 4 If the amount of mitochondria, mte, is expressed as mitochondrial mass, then  $D_{mte}$  is the mass
- 1040 fraction of mitochondria in the sample. If mte is expressed as mitochondrial volume,  $V_{mt}$ , and the
- 1041 mass of sample,  $m_X$ , is replaced by volume of sample,  $V_X$ , then  $D_{mte}$  is the volume fraction of
- 1042 mitochondria in the sample.
- 1043 5  $mte_X = mte \cdot N_X^{-1} = C_{mte} \cdot C_{NX}^{-1}$ .
- 1044 6 Entity  $O_2$  can be replaced by other chemical entities B to study different reactions.
- 1045 7  $l_{O_2}$  and  $V$  are defined per instrument chamber as a system of constant volume (and constant
- 1046 temperature), which may be closed or open.  $l_{O_2}$  is abbreviated for  $l_{O_2,r}$ , i.e. the metabolic or internal
- 1047  $O_2$  flow of the chemical reaction r in which  $O_2$  is consumed, hence the negative stoichiometric
- 1048 number,  $\nu_{O_2} = -1$ .  $l_{O_2,r} = d_r n_{O_2} / dt \nu_{O_2}^{-1}$ . If r includes all chemical reactions in which  $O_2$  participates, then
- 1049  $d_r n_{O_2} = dn_{O_2} - d_e n_{O_2}$ , where  $dn_{O_2}$  is the change in the amount of  $O_2$  in the instrument chamber and
- 1050  $d_e n_{O_2}$  is the amount of  $O_2$  added externally to the system. At steady state, by definition  $dn_{O_2} = 0$ , hence
- 1051  $d_r n_{O_2} = -d_e n_{O_2}$ .
- 1052 8  $J_{V,O_2}$  is an experimental variable, expressed per volume of the instrument chamber.
- 1053 9  $I_{X,O_2}$  is a physiological variable, depending on the size of entity X.
- 1054 10 There are many ways to normalize for a mitochondrial marker, that are used in different experimental
- 1055 approaches: (1)  $J_{mte,O_2} = J_{V,O_2} \cdot C_{mte}^{-1}$ ; (2)  $J_{mte,O_2} = J_{V,O_2} \cdot C_{mX}^{-1} \cdot D_{mte}^{-1} = J_{mX,O_2} \cdot D_{mte}^{-1}$ ; (3)  $J_{mte,O_2} =$
- 1056  $J_{V,O_2} \cdot C_{NX}^{-1} \cdot mte_X^{-1} = I_{X,O_2} \cdot mte_X^{-1}$ ; (4)  $J_{mte,O_2} = l_{O_2} \cdot mte^{-1}$ .
- 1057
- 1058
- 1059
- 1060
- 1061



1062

| Symbol        | Definition [Units]  |
|---------------|---|
| $C_{mte}$     | Mitochondrial concentration in chamber [ $x_{mte} \cdot L^{-1}$ ]           |
| $C_m$         | Sample mass concentration in chamber [ $g \cdot L^{-1}$ ]                   |
| $D_{mte}$     | Specific mte-density per tissue mass [ $x_{mte} \cdot g^{-1}$ ]             |
| $J_{m,O_2}$   | Mass-specific $O_2$ flux [ $nmol \cdot s^{-1} \cdot g^{-1}$ ]               |
| $J_{mte,O_2}$ | Mitochondria-specific $O_2$ flux [ $nmol \cdot s^{-1} \cdot x_{mte}^{-1}$ ] |
| $mte$         | Amount of mitochondrial elements [ $x_{mte}$ ]                              |
| $m_{thom}$    | Mass of tissue in the homogenate [g]  |
| $Y_{mt}$      | Yield of isolated mitochondria  |

**Respirometer chamber**

Homogenate

$v_{thom,1}$

$V$

$$C_m = C_{m,thom} \frac{v_{thom,1}}{V}$$

$$C_{mte} = C_m \cdot D_{mte}$$

$$J_{m,O_2} = \frac{J_{V,O_2}}{C_m}$$

$$J_{mte,O_2} = \frac{J_{m,O_2}}{D_{mte}}$$

1063

1064

1065

1066

1067

1068

1069

1070

1071

1072

**Fig. 8. Normalization of volume-specific flux of isolated mitochondria and tissue**

**homogenate. A:** Mitochondrial yield,  $Y_{mt}$ , in preparation of isolated mitochondria.  $v_{thom,1}$

and  $v_{stock,1}$  are the volumes transferred from the total volume,  $V_{thom}$  and  $V_{stock}$ , respectively.

$mte_{thom,1}$  is the amount of mitochondrial elements in volume  $v_{thom,1}$  used for isolation. **B:**

In respirometry with homogenate,  $v_{thom,1}$  is transferred directly into the respirometer

chamber. See **Table 6** for further explanation of symbols.

1073  
1074

**Table 7. Some useful abbreviations  
of various sample types, X.**

| Identity of sample         | X      |
|----------------------------|--------|
| Mitochondrial preparations | mtprep |
| Isolated mitochondria      | imt    |
| Tissue homogenate          | thom   |
| Permeabilized tissue       | pti    |
| Permeabilized fibres       | pfi    |
| Permeabilized cells        | pce    |
| Cells                      | ce     |

1075

1076 **Number concentration,  $C_{NX}$ :** The experimental *number concentration* of sample in the  
1077 case of cells or animals, *e.g.*, nematodes is  $C_{NX}=N_X/V$  [ $x \cdot \text{mL}^{-1}$ ], where  $N_X$  is the number of cells  
1078 or organisms in the chamber (**Table 6**).

1079 **Flow per sample entity,  $I_{X,O_2}$ :** A special case of normalization is encountered in  
1080 respiratory studies with permeabilized (or intact) cells. If respiration is expressed per cell, the  
1081  $O_2$  flow per measurement system is replaced by the  $O_2$  flow per cell,  $I_{\text{cell},O_2}$  (**Table 6**).  $O_2$  flow  
1082 can be calculated from volume-specific  $O_2$  flux,  $J_{V,O_2}$  [ $\text{nmol} \cdot \text{s}^{-1} \cdot \text{L}^{-1}$ ] (per  $V$  of the measurement  
1083 chamber [L]), divided by the number concentration of cells,  $C_{N_{ce}}=N_{ce}/V$  [ $\text{cell} \cdot \text{L}^{-1}$ ], where  $N_{ce}$  is  
1084 the number of cells in the chamber. Cellular  $O_2$  flow can be compared between cells of identical  
1085 size. To take into account changes and differences in cell size, further normalization is required  
1086 to obtain cell size-specific or mitochondrial marker-specific  $O_2$  flux (Renner *et al.* 2003).

1087 The complexity changes when the sample is a whole organism studied as an experimental  
1088 model. The well-established scaling law in respiratory physiology reveals a strong interaction  
1089 of  $O_2$  consumption and individual body mass of an organism, since *basal* metabolic rate (flow)  
1090 does not increase linearly with body mass, whereas *maximum* mass-specific  $O_2$  flux,  $\dot{V}_{O_{2\max}}$  or  
1091  $\dot{V}_{O_{2\text{peak}}}$ , is approximately constant across a large range of individual body mass (Weibel and  
1092 Hoppeler 2005), with individuals, breeds, and certain species deviating substantially from this

1093 general relationship.  $\dot{V}_{O_{2peak}}$  of human endurance athletes is 60 to 80 mL  $O_2 \cdot \text{min}^{-1} \cdot \text{kg}^{-1}$  body  
1094 mass, converted to  $J_{m,O_{2peak}}$  of 45 to 60  $\text{nmol} \cdot \text{s}^{-1} \cdot \text{g}^{-1}$  (Gnaiger 2014; **Table 8**).

1095

#### 1096 *4.3. Normalization for mitochondrial content*

1097 Normalization is a problematic subject and it is essential to consider the question of the  
1098 study. If the study aims to compare tissue performance, such as the effects of a certain treatment  
1099 on a specific tissue, then normalization can be successful, using tissue mass or protein content,  
1100 for example. If the aim, however, is to find differences of mitochondrial function independent  
1101 of mitochondrial density (**Table 6**), then normalization to a mitochondrial marker is imperative.  
1102 However, one cannot assume that quantitative changes in various markers such as  
1103 mitochondrial proteins necessarily occur in parallel with one another. It is important to first  
1104 establish that the marker chosen is not selectively altered by the performed treatment. In  
1105 conclusion, the normalization must reflect the question under investigation to reach a satisfying  
1106 answer. On the other hand, the goal of comparing results across projects and institutions  
1107 requires some standardization on normalization for entry into a databank.

1108 **Mitochondrial concentration,  $C_{mte}$ , and mitochondrial markers:** It is important that  
1109 mitochondrial content in the tissue and the measurement chamber be quantified, as a  
1110 physiological output and result of mitochondrial biogenesis and degradation, and as a quantity  
1111 for normalization in functional analyses. Mitochondrial organelles comprise a cellular  
1112 reticulum that is in a continual flux of fusion and fission. Hence the definition of an "amount"  
1113 of mitochondria is often misconceived: mitochondria cannot be counted as a number of  
1114 occurring elements. Therefore, quantification of the "amount" of mitochondria depends on  
1115 measurement of chosen mitochondrial markers. 'Mitochondria are the structural and functional  
1116 elemental units of cell respiration' (Gnaiger 2014). The quantity of a mitochondrial marker can  
1117 be considered as the measurement of the amount of *elemental mitochondrial units* or  
1118 *mitochondrial elements*, mte. However, since mitochondrial quality changes under certain

1119 stimuli, particularly in mitochondrial dysfunction, some markers can vary while other markers  
 1120 are unchanged. (1) Mitochondrial volume or membrane area are structural markers, whereas  
 1121 mitochondrial protein mass is frequently used as a marker for isolated mitochondria. (2)  
 1122 Molecular and enzymatic mitochondrial markers (amounts or activities) can be selected as  
 1123 matrix markers, *e.g.*, citrate synthase activity, mtDNA; or inner mt-membrane markers, *e.g.*,  
 1124 cytochrome *c* oxidase activity, *aa<sub>3</sub>* content, cardiolipin, TOM20. (3) Extending the  
 1125 measurement of mitochondrial marker enzyme activity to mitochondrial pathway capacity,  
 1126 measured as ET or OXPHOS capacity, can be considered as an integrative functional  
 1127 mitochondrial marker.

1128 Depending on the type of mitochondrial marker, the mitochondrial elements, *mte*, are  
 1129 expressed in marker-specific units. Although concentration and density are used synonymously  
 1130 in physical chemistry, it is recommended to distinguish *experimental mitochondrial*  
 1131 *concentration*,  $C_{mte} = mte/V$  and *physiological mitochondrial density*,  $D_{mte} = mte/m_X$ . Then  
 1132 mitochondrial density is the amount of mitochondrial elements per mass of tissue. The former  
 1133 is mitochondrial density multiplied by sample mass concentration,  $C_{mte} = D_{mte} \cdot C_{mX}$ , or  
 1134 mitochondrial content multiplied by sample number concentration,  $C_{mte} = mte_X \cdot C_{NX}$  (**Table 6**).

1135 **Mitochondria-specific flux,  $J_{mte,O_2}$ :** Volume-specific metabolic  $O_2$  flux depends on: (1)  
 1136 the sample concentration in the volume of the instrument chamber,  $C_{mX}$ , or  $C_{NX}$ ; (2) the  
 1137 mitochondrial density in the sample,  $D_{mte} = mte/m_X$  or  $mte_X = mte/N_X$ ; and (3) the specific  
 1138 mitochondrial activity or performance per elemental mitochondrial unit,  $J_{mte,O_2} = J_{V,O_2}/C_{mte}$   
 1139 (**Table 6**). Obviously, the numerical results for  $J_{mte,O_2}$  vary according to the type of  
 1140 mitochondrial marker chosen for measurement of *mte* and  $C_{mte} = mte/V$ . Some problems are  
 1141 common for all mitochondrial markers: (1) Accuracy of measurement is crucial, since even a  
 1142 highly accurate and reproducible measurement of  $O_2$  flux becomes inaccurate and noisy if  
 1143 normalized for a biased and noisy measurement of a mitochondrial marker. This problem is  
 1144 acute in mitochondrial respiration because the denominators used (the mitochondrial markers)

1145 are often very small moieties whose accurate and precise determination is difficult. This  
1146 problem can be avoided when O<sub>2</sub> fluxes measured in substrate-uncoupler-inhibitor titration  
1147 protocols are normalized for flux in a defined respiratory reference state, which is used as an  
1148 *internal* marker and yields flux control ratios, *FCRs* (Fig. 7). *FCRs* are independent of any  
1149 *externally* measured markers and, therefore, are statistically very robust. *FCRs* indicate  
1150 qualitative changes of mitochondrial respiratory control, with highest quantitative resolution,  
1151 separating the effect of mitochondrial density or concentration on  $J_{mX,O_2}$  or  $I_{X,O_2}$  from that of  
1152 function per elemental mitochondrial marker,  $J_{mte,O_2}$  (Pesta *et al.* 2011; Gnaiger 2014). (2) If  
1153 mitochondrial quality does not change and only the amount of mitochondria, defined by the  
1154 chosen mitochondrial marker, varies as a determinant of mass-specific flux, then any marker is  
1155 equally qualified in principle; then in practice selection of the optimum marker depends only  
1156 on the accuracy and precision of measurement of the mitochondrial marker. (3) If mitochondrial  
1157 flux control ratios change, then there may not be any best mitochondrial marker. In general,  
1158 measurement of multiple mitochondrial markers enables a comparison and evaluation of  
1159 normalization for a variety of mitochondrial markers.

1160

#### 1161 4.4. Evaluation of mitochondrial markers

1162 Different methods are implicated in quantification of mitochondrial markers and have  
1163 different strengths. Evaluation of mitochondrial markers in healthy controls is insufficient for  
1164 providing guidelines for application in the diagnosis of pathological states and specific  
1165 treatments. In line with the concept of the respiratory control ratio (Chance and Williams  
1166 1955a), the most readily used normalization is that of flux control ratios and flux control factors  
1167 (Gnaiger 2014). Selection of the state of maximum flux in a protocol as the reference state has  
1168 the advantages of (1) internal normalization, (2) statistical linearization of the response in the  
1169 range of 0 to 1, and (3) consideration of maximum flux for integrating a very large number of  
1170 elemental steps in the OXPHOS or ET-pathways. This reduces the risk of selecting a functional

1171 marker that is specifically altered by the treatment or pathology, yet increases the chance that  
1172 the highly integrative state is actually affected when compared with the controls. In this case,  
1173 additional information can be obtained by reporting flux control ratios based on a reference  
1174 state which indicates stable tissue-mass specific flux, *e.g.* the OXPHOS rather than ET state.  
1175 Stereological determination of mitochondrial content via two-dimensional transmission  
1176 electron microscopy can have limitations due to the dynamics of mitochondrial size (Meinild  
1177 Lundby *et al.* 2017). Accurate determination of three-dimensional volume by two-dimensional  
1178 microscopy can be both time consuming and statistically challenging (Larsen *et al.* 2012).  
1179 Using mitochondrial marker enzymes (citrate synthase activity, Complex I–IV amount or  
1180 activity) for normalization of flux is limited in part by the same factors that apply to the use of  
1181 flux control ratios. Strong correlations between various mitochondrial markers and citrate  
1182 synthase activity [1, 11, 12] are expected in a specific tissue of healthy subjects. Citrate synthase  
1183 activity has been shown to be acutely modifiable by exercise [13, 14]. Evaluation of  
1184 mitochondrial markers related to a selected age and sex cohort cannot be extrapolated to provide  
1185 recommendations for normalization in respirometric diagnosis of disease, in different states of  
1186 development and ageing, different cell types, tissues, and species. mtDNA normalised to nDNA  
1187 via qPCR is correlated to functional mitochondrial markers including OXPHOS and ET  
1188 capacity in some cases (Boushel *et al.* 2007; [5-7]), lack of such correlations have been reported  
1189 [2, 8, 9]. Several studies indicate a strong correlation between cardiolipin content and increase  
1190 in mitochondrial functionality with exercise [1-4], but its use as a general mitochondrial  
1191 biomarker in disease remains questionable.

1192

#### 1193 4.5. Conversion: units and normalization

1194 Many different units have been used to report the rate of oxygen consumption, OCR  
1195 (Table 8). SI base units provide the common reference for introducing the theoretical principles  
1196 (Fig. 7), and are used with appropriately chosen SI prefixes to express numerical data in the



1197 most practical format, with an effort towards unification within specific areas of application  
1198 (**Table 9**). For studies of cells, we recommend that respiration be expressed, as far as possible,  
1199 as (1) O<sub>2</sub> flux normalized for a mitochondrial marker, for separation of the effects of  
1200 mitochondrial quality and content on cell respiration (this includes *FCRs* as a normalization for  
1201 a functional mitochondrial marker); (2) O<sub>2</sub> flux in units of cell volume or mass, for comparison  
1202 of respiration of cells with different cell size (Renner *et al.* 2003) and with studies on tissue  
1203 preparations, and (3) O<sub>2</sub> flow in units of attomole (10<sup>-18</sup> mol) of O<sub>2</sub> consumed by each cell in a  
1204 second [amol·s<sup>-1</sup>·cell<sup>-1</sup>], numerically equivalent to [pmol·s<sup>-1</sup>·10<sup>-6</sup> cells]. This convention allows  
1205 information to be easily used when designing experiments in which oxygen consumption must  
1206 be considered. For example, to estimate the volume-specific O<sub>2</sub> flux in an instrument chamber  
1207 that would be expected at a particular cell number concentration, one simply needs to multiply  
1208 the flow per cell by the number of cells per volume of interest. This provides the amount of O<sub>2</sub>  
1209 [mol] consumed per time [s<sup>-1</sup>] per unit volume [L<sup>-1</sup>]. At an O<sub>2</sub> flow of 100 amol·s<sup>-1</sup>·cell<sup>-1</sup> and a  
1210 cell density of 10<sup>9</sup> cells·L<sup>-1</sup> (10<sup>6</sup> cells·mL<sup>-1</sup>), the volume-specific O<sub>2</sub> flux is 100 nmol·s<sup>-1</sup>·L<sup>-1</sup> (100  
1211 pmol·s<sup>-1</sup>·mL<sup>-1</sup>).

1212         Although volume is expressed as m<sup>3</sup> using the *SI* base unit, the litre [dm<sup>3</sup>] is the basic unit  
1213 of volume for concentration and is used for most solution chemical kinetics. If one multiplies  
1214  $I_{\text{cell},\text{O}_2}$  by  $C_{N_{\text{cell}}}$ , then the result will not only be the amount of O<sub>2</sub> [mol] consumed per time [s<sup>-1</sup>]  
1215 in one litre [L<sup>-1</sup>], but also the change in the concentration of oxygen per second (for any volume  
1216 of an ideally closed system). This is ideal for kinetic modeling as it blends with chemical rate  
1217 equations where concentrations are typically expressed in mol·L<sup>-1</sup> (Wagner *et al.* 2011). In  
1218 studies of multinuclear cells, such as differentiated skeletal muscle cells, it is easy to determine  
1219 the number of nuclei but not the total number of cells. A generalized concept, therefore, is  
1220 obtained by substituting cells by nuclei as the sample entity. This does not hold, however, for  
1221 enucleated platelets.

1222

1223 **Table 8. Conversion of various units used in respirometry and**  
 1224 **ergometry.**  $e$  is the number of electrons or reducing equivalents.  $z_B$  is the  
 1225 charge number of entity B.  
 1226

| 1 Unit   | x               | Multiplication factor | SI-Unit                            | Note |
|--|-----------------|-----------------------|------------------------------------|------|
| ng.atom O $\cdot$ s $^{-1}$                        | (2 e)           | 0.5                   | nmol O $_2$ $\cdot$ s $^{-1}$      |      |
| ng.atom O $\cdot$ min $^{-1}$                      | (2 e)           | 8.33                  | pmol O $_2$ $\cdot$ s $^{-1}$      |      |
| natom O $\cdot$ min $^{-1}$                        | (2 e)           | 8.33                  | pmol O $_2$ $\cdot$ s $^{-1}$      |      |
| nmol O $_2$ $\cdot$ min $^{-1}$                    | (4 e)           | 16.67                 | pmol O $_2$ $\cdot$ s $^{-1}$      |      |
| nmol O $_2$ $\cdot$ h $^{-1}$                      | (4 e)           | 0.2778                | pmol O $_2$ $\cdot$ s $^{-1}$      |      |
| mL O $_2$ $\cdot$ min $^{-1}$ at STPD <sup>a</sup> |                 | 0.744                 | $\mu$ mol O $_2$ $\cdot$ s $^{-1}$ | 1    |
| W = J/s at -470 kJ/mol O $_2$                      |                 | -2.128                | $\mu$ mol O $_2$ $\cdot$ s $^{-1}$ |      |
| mA = mC $\cdot$ s $^{-1}$                          | ( $z_{H^+}=1$ ) | 10.36                 | nmol H $^+$ $\cdot$ s $^{-1}$      | 2    |
| mA = mC $\cdot$ s $^{-1}$                          | ( $z_{O_2}=4$ ) | 2.59                  | nmol O $_2$ $\cdot$ s $^{-1}$      | 2    |
| nmol H $^+$ $\cdot$ s $^{-1}$                      | ( $z_{H^+}=1$ ) | 0.09649               | mA                                 | 3    |
| nmol O $_2$ $\cdot$ s $^{-1}$                      | ( $z_{O_2}=4$ ) | 0.38594               | mA                                 | 3    |

1227  
 1228 1 At standard temperature and pressure dry (STPD: 0 °C=273.15 K and 1  
 1229 atm=101.325 kPa=760 mmHg), the molar volume of an ideal gas,  $V_m$ , and  $V_{m,O_2}$   
 1230 is 22.414 and 22.392 L $\cdot$ mol $^{-1}$  respectively. Rounded to three decimal places, both  
 1231 values yield the conversion factor of 0.744. For comparison at NTPD (20 °C),  
 1232  $V_{m,O_2}$  is 24.038 L $\cdot$ mol $^{-1}$ . Note that the SI standard pressure is 100 kPa.

1233 2 The multiplication factor is  $10^6/(z_B \cdot F)$ .

1234 3 The multiplication factor is  $z_B \cdot F/10^6$ .

1235

#### 1236 4.5. Conversion: oxygen, proton and ATP flux

1237  $J_{O_2,k}$  is coupled in mitochondrial steady states to proton cycling,  $J_{\infty H^+} = J_{H^+,out} = J_{H^+,in}$  (**Fig.**  
 1238 **2**).  $J_{H^+,out/n}$  and  $J_{H^+,in/n}$  [nmol $\cdot$ s $^{-1}$  $\cdot$ L $^{-1}$ ] are converted into electrical units,  $J_{H^+,out/e}$   
 1239 [mC $\cdot$ s $^{-1}$  $\cdot$ L $^{-1}$ =mA $\cdot$ L $^{-1}$ ] =  $J_{H^+,out/n}$  [nmol $\cdot$ s $^{-1}$  $\cdot$ L $^{-1}$ ] $\cdot$ F [C $\cdot$ mol $^{-1}$ ] $\cdot$ 10 $^{-6}$  (**Table 4**). At a  $J_{H^+,out}/J_{O_2,k}$  ratio

1240 or  $H^+_{out}/O_2$  of 20 ( $H^+_{out}/O=10$ ), a volume-specific  $O_2$  flux of  $100 \text{ nmol}\cdot\text{s}^{-1}\cdot\text{L}^{-1}$  would correspond  
 1241 to a proton flux of  $2,000 \text{ nmol H}^+_{out}\cdot\text{s}^{-1}\cdot\text{L}^{-1}$  or volume-specific current of  $193 \text{ mA}\cdot\text{L}^{-1}$ .

$$1242 \quad J_{V,H+out/e} [\text{mA}\cdot\text{L}^{-1}] = J_{V,H+out/n} \cdot F \cdot 10^{-6} [\text{nmol}\cdot\text{s}^{-1}\cdot\text{L}^{-1} \cdot \text{mC}\cdot\text{nmol}^{-1}] \quad (\text{Eq. 3.1})$$

$$1243 \quad J_{V,H+out/e} [\text{mA}\cdot\text{L}^{-1}] = J_{V,O_2} \cdot (H^+_{out}/O_2) \cdot F \cdot 10^{-6} [\text{mC}\cdot\text{s}^{-1}\cdot\text{L}^{-1} = \text{mA}\cdot\text{L}^{-1}] \quad (\text{Eq. 3.2})$$

1244

1245 **Table 9. Conversion for units with preservation of numerical values.**

| Name   | Frequently used unit                                       | Equivalent unit                                      | Note |
|--|--|--|------|
| Volume-specific flux, $J_{V,O_2}$              | $\text{pmol}\cdot\text{s}^{-1}\cdot\text{mL}^{-1}$         | $\text{nmol}\cdot\text{s}^{-1}\cdot\text{L}^{-1}$    | 1    |
|  | $\text{mmol}\cdot\text{s}^{-1}\cdot\text{L}^{-1}$          | $\text{mol}\cdot\text{s}^{-1}\cdot\text{m}^{-3}$     |      |
| Cell-specific flow, $I_{O_2}$                  | $\text{pmol}\cdot\text{s}^{-1}\cdot 10^{-6} \text{ cells}$ | $\text{amol}\cdot\text{s}^{-1}\cdot\text{cell}^{-1}$ | 2    |
|  | $\text{pmol}\cdot\text{s}^{-1}\cdot 10^{-9} \text{ cells}$ | $\text{zmol}\cdot\text{s}^{-1}\cdot\text{cell}^{-1}$ | 3    |
| Cell number concentration, $C_{Nce}$           | $10^6 \text{ cells}\cdot\text{mL}^{-1}$                    | $10^9 \text{ cells}\cdot\text{L}^{-1}$               |      |
| Mitochondrial protein concentration, $C_{mte}$ | $0.1 \text{ mg}\cdot\text{mL}^{-1}$                        | $0.1 \text{ g}\cdot\text{L}^{-1}$                    |      |
| Mass-specific flux, $J_{m,O_2}$                | $\text{pmol}\cdot\text{s}^{-1}\cdot\text{mg}^{-1}$         | $\text{nmol}\cdot\text{s}^{-1}\cdot\text{g}^{-1}$    | 4    |
| Catabolic power, $P_{k,O_2}$                   | $\mu\text{W}\cdot 10^{-6} \text{ cells}$                   | $\text{pW}\cdot\text{cell}^{-1}$                     | 1    |
| Volume   | 1,000 L  | $\text{m}^3$ (1,000 kg)                              |      |
|  | L  | $\text{dm}^3$ (kg)                                   |      |
|  | mL   | $\text{cm}^3$ (g)                                    |      |
|  | $\mu\text{L}$  | $\text{mm}^3$ (mg)                                   |      |
|  | fL   | $\mu\text{m}^3$ (pg)                                 |      |
| Amount of substance concentration              | $\text{M} = \text{mol}\cdot\text{L}^{-1}$                  | $\text{mol}\cdot\text{dm}^{-3}$                      |      |

1246

1247 1 pmol: picomole =  $10^{-12}$  mol1248 2 amol: attomole =  $10^{-18}$  mol1249 3 zmol: zeptomole =  $10^{-21}$  mol1250 4 nmol: nanomole =  $10^{-9}$  mol

1251

1252 ET capacity in various human cell types including HEK 293, primary HUVEC and fibroblasts  
 1253 ranges from 50 to  $180 \text{ amol}\cdot\text{s}^{-1}\cdot\text{cell}^{-1}$ , measured in intact cells in the noncoupled state (see  
 1254 Gnaiger 2014). At  $100 \text{ amol}\cdot\text{s}^{-1}\cdot\text{cell}^{-1}$  corrected for ROX (corresponding to a catabolic power  
 1255 of  $-48 \text{ pW}\cdot\text{cell}^{-1}$ ), the current across the mt-membranes,  $I_e$ , approximates  $193 \text{ pA}\cdot\text{cell}^{-1}$  or 0.2  
 1256 nA per cell. See Rich (2003) for an extension of quantitative bioenergetics from the molecular  
 1257 to the human scale, with a transmembrane proton flux equivalent to 520 A in an adult at a  
 1258 catabolic power of -110 W. Modelling approaches illustrate the link between proton motive  
 1259 force and currents (Willis *et al.* 2016). For NADH- and succinate-linked respiration, the

1260 mechanistic P $\gg$ /O $_2$  ratio (referring to the full 4 electron reduction of O $_2$ ) is calculated at 20/3.7  
 1261 and 12/3.7, respectively (Eq. 4) equal to 5.4 and 3.3. The classical P $\gg$ /O ratios (referring to the  
 1262 2 electron reduction of 0.5 O $_2$ ) are 2.7 and 1.6 (Watt *et al.* 2010), in direct agreement with the  
 1263 measured P $\gg$ /O ratio for succinate of  $1.58 \pm 0.02$  (Gnaiger *et al.* 2000; for detailed reviews see  
 1264 Wikström and Hummer 2012; Sazanov 2015),

$$1265 \quad P_{\gg}/O_2 = (H^+_{out}/O_2)/(H^+_{in}/P_{\gg}) \quad (\text{Eq. 4})$$

1266 In summary (**Fig. 1**),

$$1267 \quad J_{V,P_{\gg}} [\text{nmol}\cdot\text{s}^{-1}\cdot\text{L}^{-1}] = J_{V,O_2}\cdot(H^+_{out}/O_2)/(H^+_{in}/P_{\gg}) \quad (\text{Eq. 5.1})$$

$$1268 \quad J_{V,P_{\gg}} [\text{nmol}\cdot\text{s}^{-1}\cdot\text{L}^{-1}] = J_{V,O_2}\cdot(P_{\gg}/O_2) \quad (\text{Eq. 5.2})$$

1269 We consider isolated mitochondria as powerhouses and proton pumps as molecular machines  
 1270 to relate experimental results to energy metabolism of the intact cell. The cellular P $\gg$ /O $_2$  based  
 1271 on oxidation of glycogen is increased by the glycolytic (fermentative) substrate-level  
 1272 phosphorylation of 3 P $\gg$ /Glyc, *i.e.*, 0.5 mol P $\gg$  for each mol O $_2$  consumed in the complete  
 1273 oxidation of a mol glycosyl unit (Glyc). Adding 0.5 to the mitochondrial P $\gg$ /O $_2$  ratio of 5.4  
 1274 yields a bioenergetic cell physiological P $\gg$ /O $_2$  ratio close to 6. Two NADH equivalents are  
 1275 formed during glycolysis and transported from the cytosol into the mitochondrial matrix, either  
 1276 by the malate-aspartate shuttle or by the glycerophosphate shuttle resulting in different  
 1277 theoretical yield of ATP generated by mitochondria, the energetic cost of which potentially  
 1278 must be taken into account. Considering also substrate-level phosphorylation in the TCA cycle,  
 1279 this high P $\gg$ /O $_2$  ratio not only reflects proton translocation and OXPHOS studied in isolation,  
 1280 but integrates mitochondrial physiology with energy transformation in the living cell (Gnaiger  
 1281 1993a).

1282

## 1283 **5. Conclusions**

1284 MitoEAGLE can serve as a gateway to better diagnose mitochondrial respiratory defects  
 1285 linked to genetic variation, age-related health risks, sex-specific mitochondrial performance,

1286 lifestyle with its effects on degenerative diseases, and thermal and chemical environment. The  
1287 present recommendations on coupling control states and rates, linked to the concept of the  
1288 protonmotive force (Part 1) will be extended in a series of reports on pathway control of  
1289 mitochondrial respiration, respiratory states in intact cells, and harmonization of experimental  
1290 procedures.

1291

---

1292 **Box 5: Mitochondrial and cell respiration**

1293 Mitochondrial and cell respiration is the process of highly exergonic and exothermic energy  
1294 transformation in which scalar redox reactions are coupled to vectorial ion translocation across  
1295 a semipermeable membrane, which separates the small volume of a bacterial cell or  
1296 mitochondrion from the larger volume of its surroundings. The electrochemical exergy can be  
1297 partially conserved in the phosphorylation of ADP to ATP or in ion pumping, or dissipated in  
1298 an electrochemical short-circuit. Respiration is thus clearly distinguished from fermentation as  
1299 the counterpart of cellular core energy metabolism. Respiration is separated in mitochondrial  
1300 preparations from the partial contribution of fermentative pathways of the intact cell. According  
1301 to this definition, residual oxygen consumption, as measured after inhibition of mitochondrial  
1302 electron transfer, does not belong to the class of catabolic reactions and is, therefore, subtracted  
1303 from total oxygen consumption to obtain baseline-corrected respiration.

---

1304

1305 The optimal choice for expressing mitochondrial and cell respiration (**Box 5**) as O<sub>2</sub> flow  
1306 per biological system, and normalization for specific tissue-markers (volume, mass, protein)  
1307 and mitochondrial markers (volume, protein, content, mtDNA, activity of marker enzymes,  
1308 respiratory reference state) is guided by the scientific question. Interpretation of the obtained  
1309 data depends critically on appropriate normalization, and therefore reporting rates merely as  
1310 nmol·s<sup>-1</sup> is discouraged, since it restricts the analysis to intra-experimental comparison of  
1311 relative (qualitative) differences. Expressing O<sub>2</sub> consumption per cell may not be possible when

1312 dealing with tissues. For studies with mitochondrial preparations, we recommend that  
1313 normalizations be provided as far as possible: (1) on a per cell basis as O<sub>2</sub> flow (a biophysical  
1314 normalization); (2) per g cell or tissue protein, or per cell or tissue mass as mass-specific O<sub>2</sub>  
1315 flux (a cellular normalization); and (3) per mitochondrial marker as mt-specific flux (a  
1316 mitochondrial normalization). With information on cell size and the use of multiple  
1317 normalizations, maximum potential information is available (Renner *et al.* 2003; Wagner *et al.*  
1318 2011; Gnaiger 2014). When using isolated mitochondria, mitochondrial protein is a frequently  
1319 applied mitochondrial marker, the use of which is basically restricted to isolated mitochondria.  
1320 Mitochondrial markers, such as citrate synthase activity as an enzymatic matrix marker, provide  
1321 a link to the tissue of origin on the basis of calculating the mitochondrial yield, *i.e.*, the fraction  
1322 of mitochondrial marker obtained from a unit mass of tissue.

1323

#### 1324 **Acknowledgements**

1325 We thank M. Beno for management assistance. Supported by COST Action CA15203  
1326 MitoEAGLE and K-Regio project MitoFit (EG).

1327 **Competing financial interests:** E.G. is founder and CEO of Oroboros Instruments, Innsbruck,  
1328 Austria.

1329

#### 1330 **6. References** (*incomplete; www links will be deleted in the final version*)

1331 Altmann R. Die Elementarorganismen und ihre Beziehungen zu den Zellen. Zweite vermehrte  
1332 Auflage. Verlag Von Veit & Comp, Leipzig 1894;160 pp. -

1333 [www.mitoeagle.org/index.php/Altmann\\_1894\\_Verlag\\_Von\\_Veit\\_%26\\_Comp](http://www.mitoeagle.org/index.php/Altmann_1894_Verlag_Von_Veit_%26_Comp)

1334 Birkedal R, Laasmaa M, Vendelin M. The location of energetic compartments affects  
1335 energetic communication in cardiomyocytes. *Front Physiol* 2014;5:376. doi:

1336 10.3389/fphys.2014.00376. eCollection 2014. PMID: 25324784

- 1337 Breton S, Beaupré HD, Stewart DT, Hoeh WR, Blier PU. The unusual system of doubly  
1338 uniparental inheritance of mtDNA: isn't one enough? Trends Genet 2007;23:465-74.
- 1339 Brown GC. Control of respiration and ATP synthesis in mammalian mitochondria and cells.  
1340 Biochem J 1992;284:1-13. - [www.mitoeagle.org/index.php/Brown\\_1992\\_Biochem\\_J](http://www.mitoeagle.org/index.php/Brown_1992_Biochem_J)
- 1341 Chance B, Williams GR. Respiratory enzymes in oxidative phosphorylation. I. Kinetics of  
1342 oxygen utilization. J Biol Chem 1955a;217:383-93. -  
1343 [http://www.mitoeagle.org/index.php/Chance\\_1955\\_J\\_Biol\\_Chem-I](http://www.mitoeagle.org/index.php/Chance_1955_J_Biol_Chem-I)
- 1344 Chance B, Williams GR. Respiratory enzymes in oxidative phosphorylation: III. The steady  
1345 state. J Biol Chem 1955b;217:409-27. -  
1346 [www.mitoeagle.org/index.php/Chance\\_1955\\_J\\_Biol\\_Chem-III](http://www.mitoeagle.org/index.php/Chance_1955_J_Biol_Chem-III)
- 1347 Chance B, Williams GR. Respiratory enzymes in oxidative phosphorylation. IV. The  
1348 respiratory chain. J Biol Chem 1955c;217:429-38. -  
1349 [www.mitoeagle.org/index.php/Chance\\_1955\\_J\\_Biol\\_Chem-IV](http://www.mitoeagle.org/index.php/Chance_1955_J_Biol_Chem-IV)
- 1350 Chance B, Williams GR. The respiratory chain and oxidative phosphorylation. Adv Enzymol  
1351 Relat Subj Biochem 1956;17:65-134. -  
1352 [www.mitoeagle.org/index.php/Chance\\_1956\\_Adv\\_Enzymol\\_Relat\\_Subj\\_Biochem](http://www.mitoeagle.org/index.php/Chance_1956_Adv_Enzymol_Relat_Subj_Biochem)
- 1353 Cobb LJ, Lee C, Xiao J, Yen K, Wong RG, Nakamura HK, Mehta HH, Gao Q, Ashur C,  
1354 Huffman DM, Wan J, Muzumdar R, Barzilai N, Cohen P. Naturally occurring  
1355 mitochondrial-derived peptides are age-dependent regulators of apoptosis, insulin  
1356 sensitivity, and inflammatory markers. Aging (Albany NY) 2016;8:796-809.
- 1357 Cohen ER, Cvitas T, Frey JG, Holmström B, Kuchitsu K, Marquardt R, Mills I, Pavese F,  
1358 Quack M, Stohner J, Strauss HL, Takami M, Thor HL. Quantities, units and symbols in  
1359 physical chemistry, IUPAC Green Book 2008;3rd Edition, 2nd Printing, IUPAC & RSC  
1360 Publishing, Cambridge. -  
1361 [www.mitoeagle.org/index.php/Cohen\\_2008\\_IUPAC\\_Green\\_Book](http://www.mitoeagle.org/index.php/Cohen_2008_IUPAC_Green_Book)

- 1362 Coopersmith J. Energy, the subtle concept. The discovery of Feynman's blocks from Leibnitz  
1363 to Einstein. Oxford University Press 2010;400 pp.
- 1364 Dai Q, Shah AA, Garde RV, Yonish BA, Zhang L, Medvitz NA, Miller SE, Hansen EL, Dunn  
1365 CN, Price TM. A truncated progesterone receptor (PR-M) localizes to the  
1366 mitochondrion and controls cellular respiration. *Mol Endocrinol* 2013;27:741-53.
- 1367 Duarte FV, Palmeira CM, Rolo AP. The role of microRNAs in mitochondria: small players  
1368 acting wide. *Genes (Basel)* 2014;5:865-86.
- 1369 Dufour S, Rousse N, Canioni P, Diolez P. Top-down control analysis of temperature effect on  
1370 oxidative phosphorylation. *Biochem J* 1996;314:743-51.
- 1371 Ernster L, Schatz G Mitochondria: a historical review. *J Cell Biol* 1981;91:227s-55s. -  
1372 [www.mitoeagle.org/index.php/Ernster\\_1981\\_J\\_Cell\\_Biol](http://www.mitoeagle.org/index.php/Ernster_1981_J_Cell_Biol)
- 1373 Estabrook RW. Mitochondrial respiratory control and the polarographic measurement of  
1374 ADP:O ratios. *Methods Enzymol* 1967;10:41-7. -  
1375 [www.mitoeagle.org/index.php/Estabrook\\_1967\\_Methods\\_Enzymol](http://www.mitoeagle.org/index.php/Estabrook_1967_Methods_Enzymol)
- 1376 Fell D. Understanding the control of metabolism. Portland Press 1997.
- 1377 Garlid KD, Semrad C, Zinchenko V. Does redox slip contribute significantly to mitochondrial  
1378 respiration? In: Schuster S, Rigoulet M, Ouhabi R, Mazat J-P (eds) *Modern trends in*  
1379 *biothermokinetics*. Plenum Press, New York, London 1993;287-93.
- 1380 Gerö D, Szabo C. Glucocorticoids suppress mitochondrial oxidant production via  
1381 upregulation of uncoupling protein 2 in hyperglycemic endothelial cells. *PLoS One*  
1382 2016;11:e0154813.
- 1383 Gnaiger E. Efficiency and power strategies under hypoxia. Is low efficiency at high glycolytic  
1384 ATP production a paradox? In: *Surviving Hypoxia: Mechanisms of Control and*  
1385 *Adaptation*. Hochachka PW, Lutz PL, Sick T, Rosenthal M, Van den Thillart G (eds.)  
1386 CRC Press, Boca Raton, Ann Arbor, London, Tokyo 1993a:77-109. -  
1387 [www.mitoeagle.org/index.php/Gnaiger\\_1993\\_Hypoxia](http://www.mitoeagle.org/index.php/Gnaiger_1993_Hypoxia)



- 1388 Gnaiger E. Nonequilibrium thermodynamics of energy transformations. Pure Appl Chem  
1389 1993b;65:1983-2002. - [www.mitoeagle.org/index.php/Gnaiger\\_1993\\_Pure\\_Appl\\_Chem](http://www.mitoeagle.org/index.php/Gnaiger_1993_Pure_Appl_Chem)
- 1390 Gnaiger E. Bioenergetics at low oxygen: dependence of respiration and phosphorylation on  
1391 oxygen and adenosine diphosphate supply. Respir Physiol 2001;128:277-97. -  
1392 [www.mitoeagle.org/index.php/Gnaiger\\_2001\\_Respir\\_Physiol](http://www.mitoeagle.org/index.php/Gnaiger_2001_Respir_Physiol)
- 1393 Gnaiger E. Mitochondrial pathways and respiratory control. An introduction to OXPHOS  
1394 analysis. 4th ed. Mitochondr Physiol Network 2014;19.12. Oroboros MiPNet  
1395 Publications, Innsbruck:80 pp. -  
1396 [www.mitoeagle.org/index.php/Gnaiger\\_2014\\_MitoPathways](http://www.mitoeagle.org/index.php/Gnaiger_2014_MitoPathways)
- 1397 Gnaiger E. Capacity of oxidative phosphorylation in human skeletal muscle. New  
1398 perspectives of mitochondrial physiology. Int J Biochem Cell Biol 2009;41:1837-45. -  
1399 [www.mitoeagle.org/index.php/Gnaiger\\_2009\\_Int\\_J\\_Biochem\\_Cell\\_Biol](http://www.mitoeagle.org/index.php/Gnaiger_2009_Int_J_Biochem_Cell_Biol)
- 1400 Gnaiger E, Méndez G, Hand SC. High phosphorylation efficiency and depression of  
1401 uncoupled respiration in mitochondria under hypoxia. Proc Natl Acad Sci USA  
1402 2000;97:11080-5. -  
1403 [www.mitoeagle.org/index.php/Gnaiger\\_2000\\_Proc\\_Natl\\_Acad\\_Sci\\_U\\_S\\_A](http://www.mitoeagle.org/index.php/Gnaiger_2000_Proc_Natl_Acad_Sci_U_S_A)
- 1404 Greggio C, Jha P, Kulkarni SS, Lagarrigue S, Broskey NT, Boutant M, Wang X, Conde  
1405 Alonso S, Ofori E, Auwerx J, Cantó C, Amati F. Enhanced respiratory chain  
1406 supercomplex formation in response to exercise in human skeletal muscle. Cell Metab  
1407 2017;25:301-11. - [http://www.mitoeagle.org/index.php/Greggio\\_2017\\_Cell\\_Metab](http://www.mitoeagle.org/index.php/Greggio_2017_Cell_Metab)
- 1408 Hofstadter DR. Gödel, Escher, Bach: An eternal golden braid. A metaphorical fugue on minds  
1409 and machines in the spirit of Lewis Carroll. Harvester Press 1979;499 pp. -  
1410 [www.mitoeagle.org/index.php/Hofstadter\\_1979\\_Harvester\\_Press](http://www.mitoeagle.org/index.php/Hofstadter_1979_Harvester_Press)
- 1411 Illaste A, Laasmaa M, Peterson P, Vendelin M. Analysis of molecular movement reveals  
1412 latticelike obstructions to diffusion in heart muscle cells. Biophys J 2012;102:739-48. -  
1413 PMID: 22385844

- 1414 Jephthina N, Beraud N, Sepp M, Birkedal R, Vendelin M. Permeabilized rat cardiomyocyte  
1415 response demonstrates intracellular origin of diffusion obstacles. *Biophys J*  
1416 2011;101:2112-21. - PMID: 22067148
- 1417 Komlódi T, Tretter L. Methylene blue stimulates substrate-level phosphorylation catalysed by  
1418 succinyl-CoA ligase in the citric acid cycle. *Neuropharmacology* 2017;123:287-98. -  
1419 [www.mitoeagle.org/index.php/Komlodi\\_2017\\_Neuropharmacology](http://www.mitoeagle.org/index.php/Komlodi_2017_Neuropharmacology)
- 1420 Larsen S, Nielsen J, Neigaard Nielsen C, Nielsen LB, Wibrand F, Stride N, Schroder HD,  
1421 Boushel RC, Helge JW, Dela F, Hey-Mogensen M. Biomarkers of mitochondrial  
1422 content in skeletal muscle of healthy young human subjects. *J Physiol* 590;2012:3349-  
1423 60. - [http://www.mitoeagle.org/index.php/Larsen\\_2012\\_J\\_Physiol](http://www.mitoeagle.org/index.php/Larsen_2012_J_Physiol)
- 1424 Lee C, Zeng J, Drew BG, Sallam T, Martin-Montalvo A, Wan J, Kim SJ, Mehta H, Hevener  
1425 AL, de Cabo R, Cohen P. The mitochondrial-derived peptide MOTS-c promotes  
1426 metabolic homeostasis and reduces obesity and insulin resistance. *Cell Metab*  
1427 2015;21:443-54.
- 1428 Lee SR, Kim HK, Song IS, Youm J, Dizon LA, Jeong SH, Ko TH, Heo HJ, Ko KS, Rhee BD,  
1429 Kim N, Han J. Glucocorticoids and their receptors: insights into specific roles in  
1430 mitochondria. *Prog Biophys Mol Biol* 2013;112:44-54.
- 1431 Lemieux H, Blier PU, Gnaiger E. Remodeling pathway control of mitochondrial respiratory  
1432 capacity by temperature in mouse heart: electron flow through the Q-junction in  
1433 permeabilized fibers. *Sci Rep* 2017;7:2840. -  
1434 [www.mitoeagle.org/index.php/Lemieux\\_2017\\_Sci\\_Rep](http://www.mitoeagle.org/index.php/Lemieux_2017_Sci_Rep)
- 1435 Lenaz G, Tioli G, Falasca AI, Genova ML. Respiratory supercomplexes in mitochondria. In:  
1436 Mechanisms of primary energy trasduction in biology. M Wikstrom (ed) Royal Society  
1437 of Chemistry Publishing, London, UK 2017:296-337 (in press)
- 1438 Margulis L. Origin of eukaryotic cells. New Haven: Yale University Press 1970.

- 1439 Meinild Lundby AK, Jacobs RA, Gehrig S, de Leur J, Hauser M, Bonne TC, Flück D,  
1440 Dandanell S, Kirk N, Kaech A, Ziegler U, Larsen S, Lundby C. Exercise training  
1441 increases skeletal muscle mitochondrial volume density by enlargement of existing  
1442 mitochondria and not de novo biogenesis. *Acta Physiol (Oxf)* 2017;[Epub ahead of  
1443 print].
- 1444 Miller GA. *The science of words*. Scientific American Library New York 1991;276 pp. -  
1445 [www.mitoeagle.org/index.php/Miller\\_1991\\_Scientific\\_American\\_Library](http://www.mitoeagle.org/index.php/Miller_1991_Scientific_American_Library)
- 1446 Mitchell P. Chemiosmotic coupling in oxidative and photosynthetic phosphorylation *Biochim*  
1447 *Biophys Acta Bioenergetics* 2011;1807:1507-38. -  
1448 <http://www.sciencedirect.com/science/article/pii/S0005272811002283>
- 1449 Mitchell P, Moyle J. Respiration-driven proton translocation in rat liver mitochondria.  
1450 *Biochem J* 1967;105:1147-62. -  
1451 [www.mitoeagle.org/index.php/Mitchell\\_1967\\_Biochem\\_J](http://www.mitoeagle.org/index.php/Mitchell_1967_Biochem_J)
- 1452 Moreno M, Giacco A, Di Munno C, Goglia F. Direct and rapid effects of 3,5-diiodo-L-  
1453 thyronine (T2). *Mol Cell Endocrinol* 2017;7207:30092-8.
- 1454 Morrow RM, Picard M, Derbeneva O, Leipzig J, McManus MJ, Gousspillou G, Barbat-Artigas  
1455 S, Dos Santos C, Hepple RT, Murdock DG, Wallace DC. Mitochondrial energy  
1456 deficiency leads to hyperproliferation of skeletal muscle mitochondria and enhanced  
1457 insulin sensitivity. *Proc Natl Acad Sci U S A* 2017;114:2705-10. -  
1458 [www.mitoeagle.org/index.php/Morrow\\_2017\\_Proc\\_Natl\\_Acad\\_Sci\\_U\\_S\\_A](http://www.mitoeagle.org/index.php/Morrow_2017_Proc_Natl_Acad_Sci_U_S_A)
- 1459 Nicholls DG, Ferguson S. *Bioenergetics 4*. Elsevier 2013.
- 1460 Paradies G, Paradies V, De Benedictis V, Ruggiero FM, Petrosillo G. Functional role of  
1461 cardiolipin in mitochondrial bioenergetics. *Biochim Biophys Acta* 2014;1837:408-17. -  
1462 [http://www.mitoeagle.org/index.php/Paradies\\_2014\\_Biochim\\_Biophys\\_Acta](http://www.mitoeagle.org/index.php/Paradies_2014_Biochim_Biophys_Acta)
- 1463 Price TM, Dai Q. The Role of a Mitochondrial Progesterone Receptor (PR-M) in  
1464 Progesterone Action. *Semin Reprod Med*. 2015;33:185-94.

- 1465 Prigogine I. Introduction to thermodynamics of irreversible processes. Interscience, New  
1466 York, 1967;3rd ed.
- 1467 Puchowicz MA, Varnes ME, Cohen BH, Friedman NR, Kerr DS, Hoppel CL. Oxidative  
1468 phosphorylation analysis: assessing the integrated functional activity of human skeletal  
1469 muscle mitochondria – case studies. *Mitochondrion* 2004;4:377-85. -  
1470 [www.mitoeagle.org/index.php/Puchowicz\\_2004\\_Mitochondrion](http://www.mitoeagle.org/index.php/Puchowicz_2004_Mitochondrion)
- 1471 P. M. Quiros, A. Mottis, and J. Auwerx. Mitonuclear communication in homeostasis and  
1472 stress. *Nat Rev Mol Cell Biol* 2016;17:213-26.
- 1473 Renner K, Amberger A, Konwalinka G, Gnaiger E. Changes of mitochondrial respiration,  
1474 mitochondrial content and cell size after induction of apoptosis in leukemia cells.  
1475 *Biochim Biophys Acta* 2003;1642:115-23. -  
1476 [www.mitoeagle.org/index.php/Renner\\_2003\\_Biochim\\_Biophys\\_Acta](http://www.mitoeagle.org/index.php/Renner_2003_Biochim_Biophys_Acta)
- 1477 Rich P. Chemiosmotic coupling: The cost of living. *Nature* 2003;421:583. -  
1478 [www.mitoeagle.org/index.php/Rich\\_2003\\_Nature](http://www.mitoeagle.org/index.php/Rich_2003_Nature)
- 1479 Rostovtseva TK, Sheldon KL, Hassanzadeh E, Monge C, Saks V, Bezrukov SM, Sackett DL.  
1480 Tubulin binding blocks mitochondrial voltage-dependent anion channel and regulates  
1481 respiration. *Proc Natl Acad Sci USA* 2008;105:18746-51. -  
1482 [www.mitoeagle.org/index.php/Rostovtseva\\_2008\\_Proc\\_Natl\\_Acad\\_Sci\\_U\\_S\\_A](http://www.mitoeagle.org/index.php/Rostovtseva_2008_Proc_Natl_Acad_Sci_U_S_A)
- 1483 Rustin P, Parfait B, Chretien D, Bourgeron T, Djouadi F, Bastin J, Rötig A, Munnich A.  
1484 Fluxes of nicotinamide adenine dinucleotides through mitochondrial membranes in  
1485 human cultured cells. *J Biol Chem* 1996;271:14785-90.
- 1486 Saks VA, Veksler VI, Kuznetsov AV, Kay L, Sikk P, Tiivel T, Tranqui L, Olivares J, Winkler  
1487 K, Wiedemann F, Kunz WS. Permeabilised cell and skinned fiber techniques in studies  
1488 of mitochondrial function in vivo. *Mol Cell Biochem* 1998;184:81-100. -  
1489 [http://www.mitoeagle.org/index.php/Saks\\_1998\\_Mol\\_Cell\\_Biochem](http://www.mitoeagle.org/index.php/Saks_1998_Mol_Cell_Biochem)

- 1490 Salabei JK, Gibb AA, Hill BG. Comprehensive measurement of respiratory activity in  
1491 permeabilized cells using extracellular flux analysis. *Nat Protoc* 2014;9:421-38.
- 1492 Sazanov LA. A giant molecular proton pump: structure and mechanism of respiratory  
1493 complex I. *Nat Rev Mol Cell Biol* 2015;16:375-88. -  
1494 [www.mitoeagle.org/index.php/Sazanov\\_2015\\_Nat\\_Rev\\_Mol\\_Cell\\_Biol](http://www.mitoeagle.org/index.php/Sazanov_2015_Nat_Rev_Mol_Cell_Biol)
- 1495 Schönfeld P, Dymkowska D, Wojtczak L. Acyl-CoA-induced generation of reactive oxygen  
1496 species in mitochondrial preparations is due to the presence of peroxisomes. *Free Radic*  
1497 *Biol Med* 2009;47:503-9.
- 1498 Schrödinger E. What is life? The physical aspect of the living cell. Cambridge Univ Press,  
1499 1944. - [www.mitoeagle.org/index.php/Gnaiger\\_1994\\_BTK](http://www.mitoeagle.org/index.php/Gnaiger_1994_BTK)
- 1500 Simson P, Jepihhina N, Laasmaa M, Peterson P, Birkedal R, Vendelin M. Restricted ADP  
1501 movement in cardiomyocytes: Cytosolic diffusion obstacles are complemented with a  
1502 small number of open mitochondrial voltage-dependent anion channels. *J Mol Cell*  
1503 *Cardiol* 2016;97:197-203. - PMID: 27261153
- 1504 Stucki JW, Ineichen EA. Energy dissipation by calcium recycling and the efficiency of  
1505 calcium transport in rat-liver mitochondria. *Eur J Biochem* 1974;48:365-75.
- 1506 Wagner BA, Venkataraman S, Buettner GR. The rate of oxygen utilization by cells. *Free*  
1507 *Radic Biol Med*. 2011;51:700-712.  
1508 <http://dx.doi.org/10.1016/j.freeradbiomed.2011.05.024> PMID: PMC3147247
- 1509 Watt IN, Montgomery MG, Runswick MJ, Leslie AG, Walker JE. Bioenergetic cost of  
1510 making an adenosine triphosphate molecule in animal mitochondria. *Proc Natl Acad Sci*  
1511 *U S A* 2010;107:16823-7. -  
1512 [www.mitoeagle.org/index.php/Watt\\_2010\\_Proc\\_Natl\\_Acad\\_Sci\\_U\\_S\\_A](http://www.mitoeagle.org/index.php/Watt_2010_Proc_Natl_Acad_Sci_U_S_A)
- 1513 Weibel ER, Hoppeler H. Exercise-induced maximal metabolic rate scales with muscle aerobic  
1514 capacity. *J Exp Biol* 2005;208:1635-44.

- 1515 Wikström M, Hummer G. Stoichiometry of proton translocation by respiratory complex I and  
1516 its mechanistic implications. Proc Natl Acad Sci U S A 2012;109:4431-6. -  
1517 [www.mitoeagle.org/index.php/Wikstroem\\_2012\\_Proc\\_Natl\\_Acad\\_Sci\\_U\\_S\\_A](http://www.mitoeagle.org/index.php/Wikstroem_2012_Proc_Natl_Acad_Sci_U_S_A)  
1518 Willis WT, Jackman MR, Messer JI, Kuzmiak-Glancy S, Glancy B. A simple hydraulic  
1519 analog model of oxidative phosphorylation. Med Sci Sports Exerc. 2016;48:990-1000.